



Description of *Khamul*, gen. n. (Hymenoptera: Chalcidoidea: Eurytomidae), with a hypothesis of its phylogenetic placement

M. W. GATES

Systematic Entomology Laboratory, USDA, ARS, PSI, c/o National Museum of Natural History, Washington, D. C. 20013-7012, USA.
E-mail: michael.gates@ars.usda.gov

Table of contents

Abstract	1
Introduction	1
Methods	2
Results and discussion	23
<i>Khamul</i> n. gen.	24
Key to species of <i>Khamul</i>	25
<i>Khamul erwini</i> Gates, n. sp.	26
<i>Khamul gothmogi</i> Gates, n. sp.	28
<i>Khamul lanceolatus</i> Gates, n. sp.	29
<i>Khamul tolkeini</i> Gates, n. sp.	30
Acknowledgements	31
Literature cited	31

Abstract

Khamul n. gen., a distinctive eurytomid in the subfamily Eurytominae is described from the Neotropics based upon the type species, *K. erwini*, n. sp. A hypothesis of its phylogenetic placement within Eurytominae is presented, and four new species are described: *K. erwini*, *K. gothmogi*, *K. lanceolatus*, and *K. tolkeini*. Diagnostic features are included to distinguish this taxon from other eurytomines and a key to species presented. Its biology is unknown, but label data indicate walking stick eggs (*Prisopus* sp.; Phasmatodea: Prisopodidae) as a possible host.

Key words: *Khamul*, *erwini*, *gothmogi*, *lanceolatus*, *tolkeini*, Chalcidoidea, Eurytomidae, Eurytominae, systematics

Introduction

The biology, phylogeny, and diversity of the Eurytomidae (Hymenoptera: Chalcidoidea) have been discussed recently (Campbell *et al.* 2000, Gates & Hanson 2006, Gates 2008, Lotfalizadeh *et al.* 2007). In this paper, I focus on the placement of a new genus described herein within the subfamily Eurytominae. As such, the primary goal is to assess the monophyly of the proposed new genus rather than to rework the large morphological phylogenetic treatment of Eurytominae recently put forward by Lotfalizadeh *et al.* (2007). Most eurytomines are primary or secondary parasitoids, but there are several strictly phytophagous genera. Those that are primary parasitoids typically attack eggs, larvae, or pupae of Orthoptera, Coleoptera, Diptera, and Hymenoptera (Goulet & Huber 1993; DiGiulio 1997; Noyes 2003). The hyperparasitic eurytomines often

attack primary ichneumonoid parasites. Phytophagous eurytomines are known from at least ten plant families (Zerova 1978) and are miners, galls, or seed predators. Certain eurytomines are also known to switch to phytophagy before and/or after consuming an insect host (Philips 1917, 1927).

The research presented here is based primarily upon material collected by Terry Erwin and colleagues between 1994–1999 in Ecuador using canopy fogging techniques (Erwin *et al.* 2005). This material is exceptionally rich in Chalcidoidea and contains many new species and genera. Additional material originated from Mike Sharkey and colleagues' Colombian biodiversity project, the collections of the Universidad de Costa Rica, and Instituto Nacional de Biodiversidad, Costa Rica.

In this paper, *Khamul*, n. gen. and four new species are described. I discuss character evolution based on hypothesized relationships and their potential use for further analyses within Eurytominae.

Methods

Specimen examination and preparation: Specimens in ethanol were dehydrated through ethanol and HMDS (Heraty & Hawks 1998) before point or card mounting. Images of specimens were produced by scanning electron microscopy (SEM) and an EntoVision Imaging Suite. A Nikon SMZ1500 stereomicroscope with 10X oculars (Nikon C-W10X/22) and a Chiu Technical Corp. Lumina 1 FO-150 fiber optic light source were used for card- and point-mounted specimen observation. Mylar film was placed over the ends of the light source to reduce glare from the specimen. Scanning electron microscope (SEM) images were taken with an Amray 1810 (LaB₆ source). Some specimens were cleaned of external debris with bleach and distilled water after Bolte (1996) and affixed to 12.7 X 3.2 mm Leica/Cambridge aluminum SEM stubs with carbon adhesive tabs (Electron Microscopy Sciences, #77825-12). Stub-mounted specimens were sputter coated using a Cressington Scientific 108 Auto with a gold-palladium mixture from at least three different angles to ensure complete coverage (~20–30nm coating). *Khamul lanceolatus*, n. sp., was coated in gold only, imaged via SEM, and the gold subsequently removed by soaking in a 10% potassium cyanide solution (Sela & Boyde 1977). Wing and habitus images were obtained using an EntoVision Imaging Suite, which includes a firewire JVC KY-75 3CCD digital camera mounted to a Leica M16 zoom lens via a Leica z-step microscope stand. This system fed image data to a desktop computer where Cartograph 5.6.0 (Microvision Instruments, France) was used to capture a fixed number of focal planes (based on magnification); the resulting focal planes were merged into a single, in-focus composite image. Lighting was achieved using an LED illumination dome with all four quadrants set to 99.6% intensity. The habitus illustration (Fig. 1) was produced by incorporating data from SEM and Visionary Digital source images onto a vector outline of the wasp created in Adobe Illustrator CS2. This framework subsequently was rendered digitally in Photoshop CS2 according to artistic principles concerning light and shadow with overlain SEMs serving as guide.

Terminology for surface sculpturing follows Harris (1979) and for morphology, Gibson (1997) and Lotfalizadeh *et al.* (2007). One morphological abbreviation that is not used by Gibson (1997) is on Figs. 22, 26, *scutellar boss*, **scb**. Body lengths were measured as outlined in Gates *et al.* (2006). Abbreviations used are: HTE (eye height), msp (malar space), ITS (intertorular space), LFP (lateral formaminal plate; Figs. 70, 73), PGG (postgenal groove; Fig. 39), PGL (postgenal lamina; Fig. 39), PGB (postgenal bridge; Fig. 39), and OOL (ocell-ocular distance). Specimen with data labels similar to, COSTA RICA INBIOCRI000645008 (numeric suffix differs), have been barcoded by INBio. Figures published in Lotfalizadeh *et al.* (2007) but referred to herein are cited with a lower case f (i.e., fig. 115).

Depositories: Specimens used in this study are from the National Museum of Natural History, Smithsonian Institution, Washington, D.C., USA (USNM); Museo de Insectos, Universidad de Costa Rica, Ciudad Universitaria, Costa Rica (MZCR); Coleção Sistemática da Entomologia, Instituto Nacional de Pesquisas da Amazonia, Manaus, Amazonas, Brazil (INPA); Instituto Alexander von Humboldt, Bogotá, Colombia

(IAVH), Canadian National Collection of Insects, Ottawa, Ontario (CNCI), and Instituto Nacional de Biodiversidad, Santo Domingo de Heredia, Costa Rica (INBio). Materials from Ecuador are held on indefinite loan from Escuela Polytechnica Nacional, Quito, Ecuador (EPNC).



FIGURE 1. Lateral habitus *Khamul erwini* (female).

Parsimony analysis: I explored the tree space defined by the data matrix utilizing a heuristic search in PAUP* ver. 4.0b10 (Swofford 2002) (1,000 random repetitions, hold = 10, branch swapping = TBR). To increase resolution of tree nodes, successive character weighting was used based on the maximum value of the rescaled consistency index in PAUP*. Bootstrap values were calculated in PAUP*, and both these and character changes on the tree were mapped using MacClade. Bremer support values were calculated using TreeRot3.0 (Sorenson 2007). Cladograms generated by PAUP* were edited in FigTree 1.1.2 and finished in

Adobe Illustrator CS2. Character polarities were based on hypotheses presented in previous cladistic works within Chalcidoidea (Bouček 1988, Bugbee 1936, Gates *et al.* 2006, Grissell 1995, Lotfalizadeh *et al.* 2007, Wijesekara 1997, Zerova 1988).

The analysis presented herein modifies an earlier matrix (Gates *et al.* 2006; available at: <http://www.mapress.com/zootaxa/2006f/zt01273p054.pdf>) to which additional characters or taxa were added or existing characters modified (below). Further taxa and characters were added based upon examination of the work of Lotfalizadeh *et al.* (2007), especially those characters supporting terminal nodes in their cladograms. Exemplar taxa sampled, representing the morphological diversity within Eurytominae, were selected to provide the basis for hypothesizing the placement of *Khamul* within the subfamily. However, the sampling and coding were not exhaustive given the primary goal of circumscribing generic limits of *Khamul* and previous work published (Lotfalizadeh *et al.* 2007). Outgroup taxa consisted of two species, *Heimbra opaca* Ashmead and *H. bicolor* Subba Rao, representing the eurytomid subfamily Heimbrinae. Unfortunately, some of the derived terminal taxa coded in the Lotfalizadeh *et al.* (2007) analysis were unavailable for study and/or represented by few/type specimens, limiting dissections. Where possible, representative replacements were utilized for morphological coding herein. The 30 ingroup taxa include three species of *Khamul* as defined herein and representatives of genera putatively related to *Khamul* (e.g., *Aximopsis* Ashmead *s.l.*, *Axima* Walker, *Philolema* Cameron *s.l.*) to assess generic concepts and hypothesize relationships among these taxa. Additionally, some of the characters coded by Lotfalizadeh *et al.* (2007) that supported apical clades in their analyses were not coded herein, while others were modified. For example, the Lotfalizadeh *et al.* (2007) coding for character 52 pertaining to the relative depth of the sulci of the PGB presents states 1 (sulci present but superficial) and 2 (sulci absent or vestigial). These might be confused when one could conceivably code superficial as vestigial or vice versa. In my coding (character 67), the sulci may be either present, vestigial, or absent (not seen in this analysis) thereby reducing subjectivity.

Cladistic analysis

A matrix of 32 taxa and 70 characters was compiled (Table 1). All characters were binary except 11 (2, 7, 18, 27, 37, 50, 57, 60, 62, 63, 68) that were three-state and five that were four-state (64–66, 69, 71). Characters 8, 9, 41–48 were excluded from the analysis as they had either been redefined and integrated elsewhere in the matrix or coded for a previous species-level analysis (Gates *et al.* 2006). Initial parsimony analysis produced one tree island ($n=286$) of 156 steps, and a strict consensus tree (Fig. 34) calculated (CI = 0.53, RI = 0.80). Successive reweighting (Fig. 35) reduced the number of trees to 13, which were a subset of the original 286 trees (CI = 0.53, RI = 0.80). Character change along the backbone of the presented consensus tree is reported primarily for apical clades. Below I list the modified and new character descriptions that replace/supplement those of Gates *et al.* (2006).

Character analysis

27. Dorsellum posterior median invagination:

0, absent (Fig. 2).

1, present, single depression (Fig. 3).

2, present, two depressions (Fig. 4).

The apomorphic condition is represented by the posterior margin of the dorsellum having a single, large pocket anterior to the anterodorsal margin of the propodeum (Fig. 3). The central area of the dorsellum often has a posteriorly protruding strip of cuticle, but this condition could not be homologized across the taxa in the analysis. The apomorphic condition is widespread among the species in the analysis and perhaps deserves further consideration as to its definition. State two is autapomorphic for *K. lanceolatus* and involves the bisection of the posterior median invagination (Fig. 4).

TABLE 1. Morphological character matrix.

Taxon	1	2	3	4	5	6	7	8	9	10	11	12	13	14	15	16	17	18	19	20	21	22	23	24	
<i>Axima diabolus</i> (Yosh. & Gibson)	0	0	0	1	0	1	1	0	1	1	1	1	1	0	0	0	1	1	0	0	1	1	1	1	
<i>Axima zabriskiei</i> Howard	0	0	0	1	1	1	1	0	1	1	1	1	1	0	0	0	0	1	0	0	1	1	1	0	
<i>Axima n. sp.</i> Ecuador	0	0	0	1	1	1	1	0	1	1	1	1	0	0	0	0	0	1	0	0	1	1	1	0	
<i>Aximopsis affinis</i> (Brues)	0	0	0	1	1	1	1	0	1	1	1	1	0	0	1	0	0	1	0	0	1	1	1	0	
<i>Aximopsis hespenheidei</i> Gates	0	0	0	1	1	1	2	1	1	1	1	1	1	0	0	2	0	2	0	0	1	1	1	0	
<i>Aximopsis morio</i> Ashmead	0	0	?	?	1	1	2	1	1	?	1	1	1	0	0	2	0	2	1	0	1	1	1	0	
<i>Aximopsis (s.l.) sp. Mesoeurytoma</i>	0	0	0	1	1	1	2	1	1	1	1	1	0	0	0	0	0	2	0	0	1	1	1	0	
<i>Aximopsis (s.l.) nodularis</i> (Boheman)	0	0	0	1	1	1	1	0	1	1	1	1	0	0	0	0	0	0	0	0	0	1	0	1	0
<i>Aximopsis vogti</i> Gates	0	0	0	1	1	1	2	1	1	1	1	1	1	0	0	2	0	2	0	0	1	1	1	0	
<i>Bephratalloides cubensis</i> (Ash.)	0	1	0	1	1	1	1	0	1	1	0	0	0	0	0	0	0	0	0	0	0	0	0	0	0
<i>Bephratoides bakeri</i> (Burks)	0	0	0	1	1	1	1	0	1	1	1	0	0	?	0	0	0	0	0	0	0	1	0	0	0
<i>Bephratoides sp.</i> Maryland	0	0	0	1	1	1	3	0	1	1	1	0	0	0	0	0	0	0	0	0	0	0	0	1	0
<i>Buresium rufum</i> Bouček	0	0	0	0	1	0	1	0	0	0	0	0	0	0	0	0	0	0	0	0	0	0	0	0	0
<i>Chryseida bennetti</i> Burks	0	0	0	1	1	1	2	0	1	1	1	1	0	0	0	0	0	0	0	0	0	1	0	1	0
<i>Chryseida sp.</i> Bolivia	0	0	0	1	1	1	2	0	1	1	1	1	0	1	0	0	0	0	0	0	0	1	1	1	0
<i>Eudoxinna transversa</i> (Walker)	0	0	0	1	1	1	1	0	1	1	1	0	0	0	0	0	0	0	0	0	0	0	0	1	0
<i>Eurytoma sp.</i> "Euglossa"	0	0	0	1	1	1	1	0	1	1	1	1	0	0	0	0	0	0	0	0	0	1	0	1	0
<i>Heimbra opaca</i> Ashmead	1	0	0	0	1	1	0	0	0	0	0	0	0	?	0	0	0	0	0	0	1	0	0	1	0
<i>Heimbra bicolor</i> Subba Rao	1	0	0	0	1	1	0	0	0	0	0	0	0	?	0	0	0	0	0	0	1	0	0	1	0
<i>Khamul erwini, n. sp.</i>	0	0	0	1	1	1	1	1	1	1	1	1	0	1	0	0	0	0	0	0	1	1	1	1	0
<i>Khamul tolkeini, n. sp.</i>	0	0	0	1	1	1	1	1	1	1	1	1	0	1	0	0	0	0	0	0	1	1	1	1	0
<i>Khamul lanceolatus, n. sp.</i>	0	0	0	1	1	1	1	1	1	1	1	1	0	1	0	0	0	0	0	0	1	1	1	1	0
<i>Macrorileya oecanthi</i> (Ash.)	1	2	0	0	1	1	1	0	0	0	0	0	0	0	0	0	0	0	0	0	0	0	0	0	0
<i>Macrorileya inopinata</i> (Silv.)	1	2	1	0	1	0	1	0	0	0	0	0	0	0	0	0	0	0	0	0	0	0	0	0	0
<i>Philolema carinigena</i> Cameron	0	0	0	1	1	1	2	0	1	?	?	1	0	1	0	0	0	0	0	0	?	1	1	0	0
<i>Philolema javensis</i> (Girault)	0	0	0	1	1	1	2	0	1	?	1	1	0	0	0	0	0	0	0	0	?	1	1	0	0
<i>Philolema latrodecti</i> (Fullaway)	0	0	0	1	1	1	2	0	1	1	1	1	0	0	0	0	0	0	0	0	0	1	1	1	0
<i>Philolema tephrosiae</i> (Girault)	0	0	0	1	1	1	2	1	1	?	?	1	0	0	0	0	0	0	0	0	?	1	?	0	0
<i>Plutarchia sp.</i> Kenya	0	0	0	1	1	1	2	1	0	1	1	1	0	0	0	0	0	0	0	0	0	0	1	1	0
<i>Systole albipennis</i> Walker	0	2	0	1	1	0	1	0	0	1	0	0	0	0	0	0	0	0	0	0	0	0	0	0	0
<i>Tenuipetiolus mentha</i> Bugbee	0	0	0	1	1	1	1	0	1	1	1	0	0	0	0	0	0	0	0	0	0	0	0	0	0
<i>Tetramesa hordei</i> (Harris)	0	0	0	1	1	1	1	0	0	0	0	0	0	0	0	0	0	0	0	0	0	0	0	0	0

continued.

Taxon	2	2	2	2	2	3	3	3	3	3	3	3	3	3	3	4	4	4	4	4	4	4	4	4	4	4	4	
	5	6	7	8	9	0	1	2	3	4	5	6	7	8	9	0	1	2	3	4	5	6	7	8				
<i>Axima diabolus</i> (Yosh. & Gibson)	0	1	1	0	1	1	1	1	1	1	1	0	2	1	?	1	1	0	1	1	0	0	1	1				
<i>Axima zabriskiei</i> Howard	0	1	1	1	1	1	1	1	1	1	1	0	1	1	0	1	1	1	1	1	1	0	0	1	1			
<i>Axima n. sp.</i> Ecuador	0	1	1	0	1	1	1	1	1	1	1	0	1	1	?	1	1	1	1	1	1	0	0	1	1			
<i>Aximopsis affinis</i> (Brues)	0	1	1	1	1	1	1	1	1	1	1	0	0	0	0	1	1	1	1	1	1	1	1	1	1			
<i>Aximopsis hespenheidei</i> Gates	0	1	1	1	1	1	1	1	1	1	1	0	0	0	1	1	1	1	1	1	1	1	1	1	1			
<i>Aximopsis morio</i> Ashmead	0	1	1	1	1	1	1	1	1	1	1	0	0	0	1	1	1	1	1	1	1	1	1	0	0			
<i>Aximopsis (s.l.) sp. Mesoeurytoma</i>	0	1	1	1	1	1	1	0	1	1	0	0	0	?	1	1	1	1	1	1	1	1	1	0				
<i>Aximopsis (s.l.) nodularis</i> (Boheman)	0	1	1	0	0	0	1	1	0	1	0	0	0	0	0	0	0	1	0	0	0	0	0	0				
<i>Aximopsis vogti</i> Gates	0	1	1	1	1	1	1	1	1	1	1	0	0	0	1	1	1	1	1	1	1	1	1	1				
<i>Bephratalloides cubensis</i> (Ash.)	0	1	1	0	0	0	0	1	0	0	0	0	0	0	0	0	0	0	0	0	0	0	0	0				
<i>Bephratoides bakeri</i> (Burks)	0	0	1	0	0	1	0	1	0	0	0	0	1	0	0	0	0	0	0	0	0	0	0	0				
<i>Bephratoides sp.</i> Maryland	0	1	1	0	0	1	?	?	0	0	?	0	0	0	?	0	0	0	0	0	0	0	0	0				
<i>Buresium rufum</i> Bouček	0	0	0	0	0	1	0	0	0	0	0	0	1	0	?	0	0	0	0	0	0	0	0	0				
<i>Chryseida bennetti</i> Burks	0	1	1	0	0	0	1	1	0	1	0	0	0	0	0	0	0	0	0	0	0	0	0	0				
<i>Chryseida sp.</i> Bolivia	0	1	1	0	0	0	1	1	0	1	0	0	0	0	0	0	0	0	0	0	0	0	0	0				
<i>Eudoxinna transversa</i> (Walker)	0	0	0	0	0	1	0	1	0	0	0	0	0	0	?	0	0	0	0	0	0	0	0	0				
<i>Eurytoma sp.</i> "Euglossa"	0	1	1	0	0	0	1	1	0	1	0	0	0	0	0	0	1	1	1	1	1	0	0	0				
<i>Heimbra opaca</i> Ashmead	1	0	0	0	0	1	0	0	0	0	0	0	0	0	?	0	0	0	0	0	0	0	0	0				
<i>Heimbra bicolor</i> Subba Rao	1	0	0	0	0	1	0	0	0	0	0	0	0	0	?	0	0	0	0	0	0	0	0	0				
<i>Khamul erwini, n. sp.</i>	0	1	1	1	0	0	1	0	0	1	1	?	0	0	0	0	0	0	0	0	0	0	0	0				
<i>Khamul tolkeini, n. sp.</i>	0	1	1	1	0	0	1	0	0	1	1	?	0	0	0	0	0	0	0	0	0	0	0	0				
<i>Khamul lanceolatus, n. sp.</i>	0	1	2	1	0	0	1	0	0	1	1	?	0	0	0	0	0	0	0	0	0	0	0	0				
<i>Macrorileya oecanthi</i> (Ash.)	0	0	0	0	0	1	0	0	0	0	0	1	0	0	0	0	0	0	0	0	0	0	0	0				
<i>Macrorileya inopinata</i> (Silv.)	0	0	0	0	0	1	0	0	0	0	0	1	0	0	?	0	0	0	0	0	0	0	1	0				
<i>Philolema carinigena</i> Cameron	0	1	1	1	1	0	1	1	0	1	1	0	0	0	?	0	0	0	0	0	0	0	0	0				
<i>Philolema javensis</i> (Girault)	0	1	1	1	1	0	1	1	0	1	1	0	0	0	?	1	0	0	0	0	0	1	1	1				
<i>Philolema latrodecti</i> (Fullaway)	0	1	1	1	1	0	1	1	0	1	1	0	0	0	0	0	0	0	0	0	0	0	0	0				
<i>Philolema tephrosiae</i> (Girault)	0	1	1	1	1	0	1	1	0	1	1	0	0	0	0	0	0	0	0	0	0	0	0	0				
<i>Plutarchia sp.</i> Kenya	0	0	1	1	1	0	0	0	0	0	0	0	0	0	?	0	0	0	0	0	0	0	0	0				
<i>Systole albipennis</i> Walker	0	0	1	0	0	0	0	0	0	1	0	0	0	0	0	0	0	0	0	0	0	0	0	0				
<i>Tenuipetiolus mentha</i> Bugbee	0	0	1	0	0	0	0	0	0	1	0	0	0	0	0	0	0	0	0	0	0	0	0	0				
<i>Tetramesa hordei</i> (Harris)	0	0	0	0	0	?	0	0	0	0	0	0	0	0	0	0	0	0	0	0	0	0	0	0				

continued.

Taxon	4	5	5	5	5	5	5	5	5	5	5	6	6	6	6	6	6	6	6	6	7	7	
	9	0	1	2	3	4	5	6	7	8	9	0	1	2	3	4	5	6	7	8	9	0	1
<i>Axima diabolus</i> (Yosh. & Gibson)	0	1	0	0	0	0	1	0	1	1	0	2	1	0	1	3	3	3	1	1	3	2	0
<i>Axima zabriskiei</i> Howard	0	2	0	0	0	0	1	0	1	1	0	2	1	0	1	3	3	3	1	1	3	2	0
<i>Axima n. sp.</i> Ecuador	0	2	0	0	0	0	1	0	1	0	0	2	1	0	1	3	3	3	1	1	3	2	0
<i>Aximopsis affinis</i> (Brues)	0	0	0	0	0	0	0	0	1	1	0	2	1	0	2	2	2	2	1	1	3	2	0
<i>Aximopsis hespenheidei</i> Gates	0	0	0	0	0	0	?	0	1	1	1	2	1	0	1	2	2	2	1	1	3	2	0
<i>Aximopsis morio</i> Ashmead	0	0	0	?	0	0	?	0	1	1	0	2	1	?	1	?	?	?	?	1	3	2	0
<i>Aximopsis (s.l.) sp. Mesoeurytoma</i>	0	0	0	0	0	0	?	0	1	1	0	2	1	0	1	2	2	1	1	1	?	2	0
<i>Aximopsis (s.l.) nodularis</i> (Boheman)	0	0	0	0	0	0	?	0	1	1	0	2	1	0	1	2	2	1	1	1	3	1	0
<i>Aximopsis vogti</i> Gates	0	0	0	0	0	0	1	0	1	1	1	2	1	0	1	2	2	2	1	1	3	2	0
<i>Bephratalloides cubensis</i> (Ash.)	0	0	0	0	0	0	1	0	2	1	0	2	1	0	2	0	2	0	0	0	1	0	0
<i>Bephratoides bakeri</i> (Burks)	0	0	0	0	0	0	?	0	0	0	0	2	1	?	?	?	?	?	?	1	3	0	0
<i>Bephratoides sp.</i> Maryland	0	0	0	0	0	0	1	0	1	0	0	2	1	0	1	1	1	1	1	1	3	0	0
<i>Buresium rufum</i> Bouček	0	0	0	0	0	0	1	0	0	1	0	0	0	0	0	3	?	0	1	0	0	0	0
<i>Chryseida bennetti</i> Burks	0	0	0	0	0	0	1	0	0	1	1	2	1	0	1	3	2	1	1	1	3	0	1
<i>Chryseida sp.</i> Bolivia	1	0	0	0	0	0	1	0	1	0	0	2	1	0	1	3	2	1	1	1	3	0	1
<i>Eudoxinna transversa</i> (Walker)	0	2	0	0	0	0	?	0	1	0	0	2	1	2	0	2	2	1	1	1	3	0	0
<i>Eurytoma sp.</i> "Euglossa"	0	0	0	0	0	0	0	0	2	1	0	2	1	0	0	3	2	1	1	1	3	1	0
<i>Heimbra opaca</i> Ashmead	0	1	0	0	0	0	1	0	0	0	0	2	0	0	0	1	0	0	0	1	3	0	0
<i>Heimbra bicolor</i> Subba Rao	0	1	0	0	0	0	1	0	0	0	0	2	0	0	0	1	0	0	0	1	3	0	0
<i>Khamul erwini</i> , n. sp.	1	2	0	1	0	1	0	1	0	0	1	2	0	1	1	1	0	0	1	1	2	0	0
<i>Khamul tolkeini</i> , n. sp.	1	2	0	1	0	1	?	1	0	0	1	2	0	1	1	?	?	?	?	1	2	0	0
<i>Khamul lanceolatus</i> , n. sp.	1	2	1	1	1	1	0	1	1	0	1	2	1	1	1	1	0	0	1	1	2	0	0
<i>Macrorileya oecanthi</i> (Ash.)	0	0	0	0	0	0	1	0	0	1	0	0	1	0	0	3	1	0	0	0	0	0	0
<i>Macrorileya inopinata</i> (Silv.)	0	0	0	0	0	0	1	0	0	1	0	0	1	0	0	3	1	0	0	0	0	0	0
<i>Philolema carinigena</i> Cameron	0	0	0	0	0	0	?	0	?	1	1	2	1	?	?	?	?	?	?	2	3	3	0
<i>Philolema javensis</i> (Girault)	0	0	0	0	0	0	?	0	2	1	1	2	1	2	1	?	?	?	?	2	3	3	0
<i>Philolema latrodecti</i> (Fullaway)	0	0	0	0	0	0	?	0	1	0	1	2	0	2	1	2	2	2	0	2	3	3	0
<i>Philolema tephrosiae</i> (Girault)	0	0	0	0	0	0	?	0	2	1	1	2	1	?	1	?	?	?	?	2	3	3	0
<i>Plutarchia sp.</i> Kenya	0	0	0	0	0	0	?	0	1	0	1	2	0	2	2	1	2	1	1	1	3	2	0
<i>Systole albipennis</i> Walker	0	0	0	0	0	0	1	0	0	1	0	1	0	0	0	2	3	3	1	0	0	0	0
<i>Tenuipetiolus mentha</i> Bugbee	0	0	0	0	0	0	1	0	2	1	0	2	0	0	0	1	2	1	1	1	0	0	0
<i>Tetramesa hordei</i> (Harris)	0	0	0	0	0	0	1	0	0	1	0	0	0	0	0	1	2	1	1	0	0	0	0

49. Flagellar segmentation:

0, flagellomeres distinctly separated, flagellar profile not parallel-sided, setation various (Figs. 5, 8, 11).

1, flagellomeres tightly appressed, flagellar profile parallel-sided, setation decumbent (Figs. 6, 7).

This character focuses on the unusual (for Eurytominae) parallel-sided flagellum. The flagellomeres of *Khamul* are cylindrical and closely appressed. Flagellomere setation is decumbent with the longest seta subequal to or less than the width of the corresponding segment (Figs. 6, 7). Many eurytomines have flagellomeres distinctly separated and setation longer than the width of the corresponding segment (Figs. 8, 11). Further, setation is more characteristically erect, though not always obviously so, and is usually decumbent to subdecumbent. The antenna of *Khamul* resembles that of many Chalcididae in gross habitus, but the setation in many chalcidids is very short, less than the length of the corresponding segment (Figs. 9, 10). Further, certain other taxa within Eurytominae possess a cylindrical flagellum very similar to that of *Khamul*, including at least two unidentified species each in *Bephratoides* and *Chryseida*.

50. Pedicel habitus:

0, Subconical in lateral view (Figs. 5, 8, 11).

1, Transverse in lateral view (Fig. 12).

2, Wedge shaped in lateral view (Fig. 13).

The conical, gradually tapering pedicel is most commonly encountered in Eurytominae. The transverse condition of state one is represented in this analysis by the outgroup Heimbrinae. State two initially was considered a synapomorphy of *Khamul*, but it is also present in *Axima diabolus* (Gibson & Yoshimoto) (Fig. 14) and *Eudoxinna transversa* Walker. A recently discovered new species of *Eudoxinna* from Costa Rica has state two as does an uncommon species of *Chryseida*, so this character will ultimately require reassessment.

51. Clypeus, separation:

0, Continuous with supraclypeal area, not separated by carina (Fig. 15).

1, Separated from supraclypeal area laterally by carina (Fig. 16).

Character state one is autapomorphic for *K. lanceolatus*.

52. Clava, apical sensilla:

0, Sensillar area at apex of clava circular (Fig. 17).

1, Sensillar area at apex of clava linear (Fig. 18).

A linear sensillar region at the apex of the clava is a putative synapomorphy supporting *Khamul erwini*, *K. tolkeini*, and *K. lanceolatus*. All other taxa in this analysis possess a circular sensillar area. A specimen fitting the definition of *Aximopsis s. l.* (Lotfalizadeh *et al.* 2007) recently was discovered in the USNM that possesses an elongate sensillar area. However, this specimen has not been examined under high magnification to assess microstructural details. Further, certain other taxa within Eurytominae possess a linear sensillar very similar to that of *Khamul*, including at least two unidentified species each in *Bephratoides* and *Chryseida*.

53. Mandible:

0, Normal, bi- or tridentate apically, outer margin curved (Fig. 19).

1, Unidentate apically, linear (Fig. 20).

The most common mandibular dentition in Eurytominae consists of 2–3 teeth. The mandibles usually are endodont, curve inwards and overlap medially when closed. In *K. lanceolatus*, the mandibles are cruciate, linear, and unidentate apically; thus, this character is autapomorphic for that taxon.

54. Notauli:

0, Complete, shallow groove (Figs. 21, 27, 79).

1, Complete, deep groove (Fig. 22).

Most eurytomines possess an indication of complete notauli. For purposes of this analysis, notauli were coded as complete – either shallow or deep. Lotfalizadeh *et al.* (2007) record other conditions within Eurytominae, including incomplete, steplike, and moderately deep and broad. Their image of the notauli of *Eurytoma aspila* (fig. 114) closely resembles the condition in *Khamul*. Thus this character is globally homoplastic

but locally informative.

55. Mesocoxal cavity:

0, Open posteriorly (Fig. 23).

1, Closed posteriorly (Fig. 24).

The sclerite surrounding the mesocoxal cavity is either open or closed in Eurytominae. In the closed condition the entire cuticular margin closely surrounds the mesocoxal opening; in the open condition the surrounding cuticle contains a narrow gap. The open condition present in two species of *Khamul* is also seen in *Aximopsis affinis* (Brues) and *Eurytoma 'Euglossa'*. Lotfalizadeh *et al.* (2007) also coded this taxon in their analysis with only the outgroup taxa (*Glyphomerus stigma* F. (fig. 166) (Torymidae) and *Lycisca* sp. (Pteromalidae)) having the open state. However, these outgroup taxa have the opening broad and membraneous as opposed to the taxa coded as open in this analysis where the gap is very narrow.

56. Scutellar boss:

0, absent (Fig. 25).

1, present (Figs. 22, 26).

The plesiomorphic character state consists of a non-elevated scutellum with a generally uniform surface sculpture throughout. In the apomorphic condition, there exists a more or less elevated subcircular area mesally on the scutellum. This area lacks the typical umbilicate punctation and is replaced by engraved reticulation. This character is unique to *Khamul* in this analysis.

57. Axillular grooves:

0, Shallow, without medial pit (Figs. 21, 27).

1, Deep, internalized medially as a pit (Figs. 28, 29).

State zero occurs most commonly in more elongate and/or smoothly sculptured eurytomid taxa (e.g., *Tetramesa*, *Buresium*, *Systole*), whereas state one appears as a deep groove or pit within a groove that is internally continuous with a linear invagination at the transscutal line. Lotfalizadeh *et al.* (2007) coded three separate axillular characters, one dealing with groove depth, another with their approximation on the transscutal line, and, finally, their degree of groove completeness (not obliterated by sculpture). I have elected not to use the approximation character of Lotfalizadeh *et al.* (2007) as degree of closeness was not objectively defined based upon relative measurement.

58. Costal cell:

0, Complete, dense row of fine setae on anterodorsal margin absent (Fig. 32).

1, Complete, dense row of fine setae on anterodorsal margin present (Figs. 30, 31, 33).

State zero may be represented by only a few longer setae on the anterodorsal margin of the costal cell, but such setation may be absent altogether. State one is indicated by a complete row of fine setae on the anterodorsal margin of the costal cell. State one typically corresponds with a dense setation on the dorsal and ventral surfaces of the costal cell, most commonly spanning the breadth of the cell, especially in the apical third to half. State one is found in *Khamul*, *Heimbria*, *Eurytoma 'Euglossa'*, *Eudoxinna transversa*, and *Aximopsis (s.l.) nodularis* in this analysis.

59. Supraclypeal area:

0, Not delimited by submedian carinae (Figs. 71, 72).

1, Delimited by submedian carinae (Fig. 38).

This character was coded by Lotfalizadeh *et al.* (2007) and supported the *Philolema* genus group, which includes rare taxa (e.g. *Ramanuja*, *Fronsona*, *Banyoma*) that are not present in the USNM, present in numbers precluding dissection, or only known from types, thus were not coded. This character is shared by *Khamul*, *Philolema*, *Plutarchia*, *C. bennetti*, and four of five *Aximopsis s.l.* in this analysis.

60. Genal carina:

0, Gena and postgena with identical sculpture, not separated by carina (Fig. 70).

1, Gena and postgena differently sculptured, sometimes slightly angulate ventrally (fig. 48).

2, Gena and postgena differently sculptured, separated by carina (Figs. 39, 73).

Lotfalizadeh *et al.* (2007) originally coded state two as separate states: gena faintly carinate posteriorly and strongly carinate posteriorly. Coding a faint versus strong carina is open to interpretation as is the homology of those two states. As this character exists as a morphocline within the various taxa of Eurytominae, delineating discrete states can be challenging.

61. Intertorular space:

0, Not produced dorsally, at most even with dorsal rim of toruli (Fig. 71).

1, Angularly produced dorsally, extending $\sim 1/4$ – $3/4$ torulus diameter above dorsal rim of toruli (Fig. 72). Six characters (20–25) directly concerning the intertorular space were coded by Lotfalizadeh *et al.* (2007) as well as an additional antennal scrobes intrascrobal lamina (27) character. It was not possible in every instance to use the images and character descriptions concerning the ITS provided by Lotfalizadeh *et al.* (2007) to accurately assess homologies or to reconstruct their character codings. This is primarily due to subjective descriptors (e.g. character 22, ITS median crest: hardly raised (state 1; fig. 31) versus evidently raised (state 2; fig. 32) and image orientation. For example, their ITS, lateral aspect character is illustrated by anterior head views (state 2) or not figured (state 3). This is important when attempting to differentiate, small tooth (state 2, in part) or rounded bump (state 3) from strongly raised rounded bump (state 4; fig. 201). I have simplified and combined two of their ITS characters into one character.

62. Postgenal depression at hypostomal/oral fossa:

0, Absent (Fig. 70).

1, Present, extends to midlength hypostomal fossa, delimited dorsally and/or laterally by ridge (Fig. 39).

2, Present, does not extend to midlength hypostomal fossa, located at oral fossa, partially delimited by ridge (Fig. 73).

The separate coding of various depressions exhibited by the postgenal region in Eurytominae (Lotfalizadeh *et al.* 2007) assumes independence among the locations of the depressions. Specifically, is a depression located at the edge of the oral fossa non-homologous with a depression located along the hypostomal fossa, or might the former simply be a reduction of the latter? Thus, I have simplified and combined the three characters used by Lotfalizadeh *et al.* (2007) for the purposes of this analysis. State 1 is unique to *Khamul* and state 2 is homoplastic, found in *Eudoxinna*, *Philolema*, and *Plutarchia*. The remaining taxa are state 0.

63. Postgenal laminae:

0, Absent.

1, Present, divergent ventrally (Fig. 39).

2, Present, convergent ventrally not reaching hypostomal carina (Fig. 74).

Postgenal laminae are often angulate lobes located at the ventral end of the PGG. These lobes are variously produced and contact the hypostomal fossa in some instances. An additional, uncommon state coded by Lotfalizadeh *et al.* (2007) has PGL convergent ventrally and reaching the hypostomal carina, however, that state was not present in taxa in this analysis. This character was modified from Lotfalizadeh *et al.* (2007) to exclude one state (PGL smoothly joining posterior margin of gena) from their PGL, orientation on lower part of PGG character. The smooth joining of the PGL to the gena does not pertain to the orientation of the PGL, but could be coded as a separate character. Their second PGL character (43) concerns its habitus, but uses descriptors such as very slightly (fig. 65), distinctly (figs. 53, 65), and strongly (figs. 51, 67), to characterize the degree of production above the surface of the postgena. Their images cited do not allow for accurate interpretation of these character states. Further, their figure 65 is used to illustrate two states, but this may be a typo. Most taxa in this analysis possess state 1, including *Khamul*, while state 2 is seen in *Plutarchia*, *B. cubensis*, and *Aximopsis affinis*.

64. Lateral foraminal plate:

0, Absent (fig. 54).

1, Present, dorsally delimited (Figs. 39, 76).

2, Present dorsally and laterally delimited, extending up to 1/2 length to tentorial pits (Fig. 73).

3, Present dorsally and laterally delimited, extending to tentorial pits (Fig. 70).

This character was slightly modified from character 44 used by Lotfalizadeh *et al.* (2007) and appears informative in separating *Aximopsis s.l.* from *Philolema s.l.* (among others). However, *Aximopsis nodularis* and *Aximopsis oryziphora* are coded as state 1 in their analysis (like *Philolema* spp.) whereas the remaining *Aximopsis* spp. are coded as state 2. This character's intraspecific variation may require some reevaluation as some taxa appear to have LFP delimited laterally (continuous with PGG or not), but are not coded as such. Other characters (45–47) coded by Lotfalizadeh *et al.* (2007) pertaining to the LFP include LFP surface that can either be absent (0), flat (1), or convex (2). I have coded both *Aximopsis* spp. and *Philolema latrodecti* as state 2 in my analysis given that the LFP are definitely produced laterally even though they may not extend quite to the distance to the tentorial pits while *Khamul* has state 1. This character was homoplastic in this analysis.

65. Postgenal bridge ornamentation:

0, Digitiform expansions of cuticle and vertical/horizontal folds present (Figs. 48, 77).

1, Only digitiform expansions of cuticle present, folds absent (Fig. 70).

2, Only vertical folds present, digitiform expansions absent (Fig. 75).

3, Absent (Fig. 78).

The plesiomorphic condition was shared by both *Heimbra* and *Khamul* in this analysis while *Axima* shared state 3 with *Systole*.

66. Postgenal bridge ornamentation strip:

0, Broad, strip width >1/3 distance between tentorial pits (Fig. 77).

1, Narrow, strip width <1/3 distance between tentorial pits (Fig. 75).

2, Vestigial (Fig. 73).

3, Absent. (Fig. 78).

The plesiomorphic condition was shared by *Heimbra* spp., *Macrorileya* spp., *Buresium rufum*, and *Khamul* spp. in this analysis while *Axima* share state 3 with *Systole*.

67. Postgenal bridge sulci:

0, Present, deep (Figs. 70, 77).

1, Vestigial, shallow, at least traceable if incomplete (Fig. 76).

Six characters were coded by Lotfalizadeh *et al.* (2007) to delineate the character states associated with the postgenal sulci. I have modified and combined two of their characters (48, 52) in order to implement a reproducible coding. Their states 'absent' and 'vestigial' should be coded separately, but were combined as one state and coded as such in five of the six characters presented by Lotfalizadeh *et al.* (2007). In this analysis, all taxa have state 1, with the exception of *B. cubensis*, *Heimbra* spp., *Macrorileya* spp., and *P. latrodecti*.

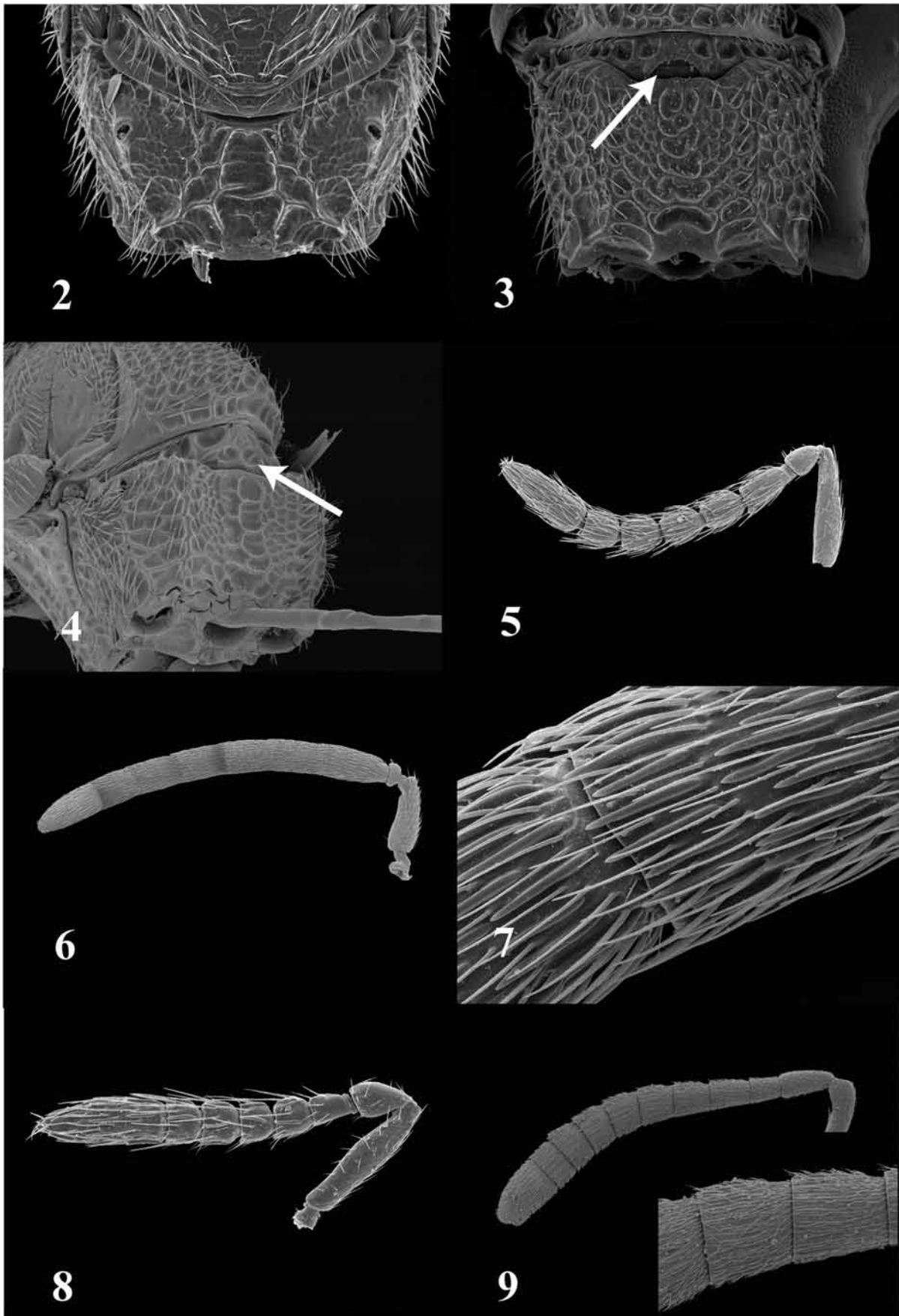
68. Mesopleuron, ventral shelf:

0, Absent (Fig. 79).

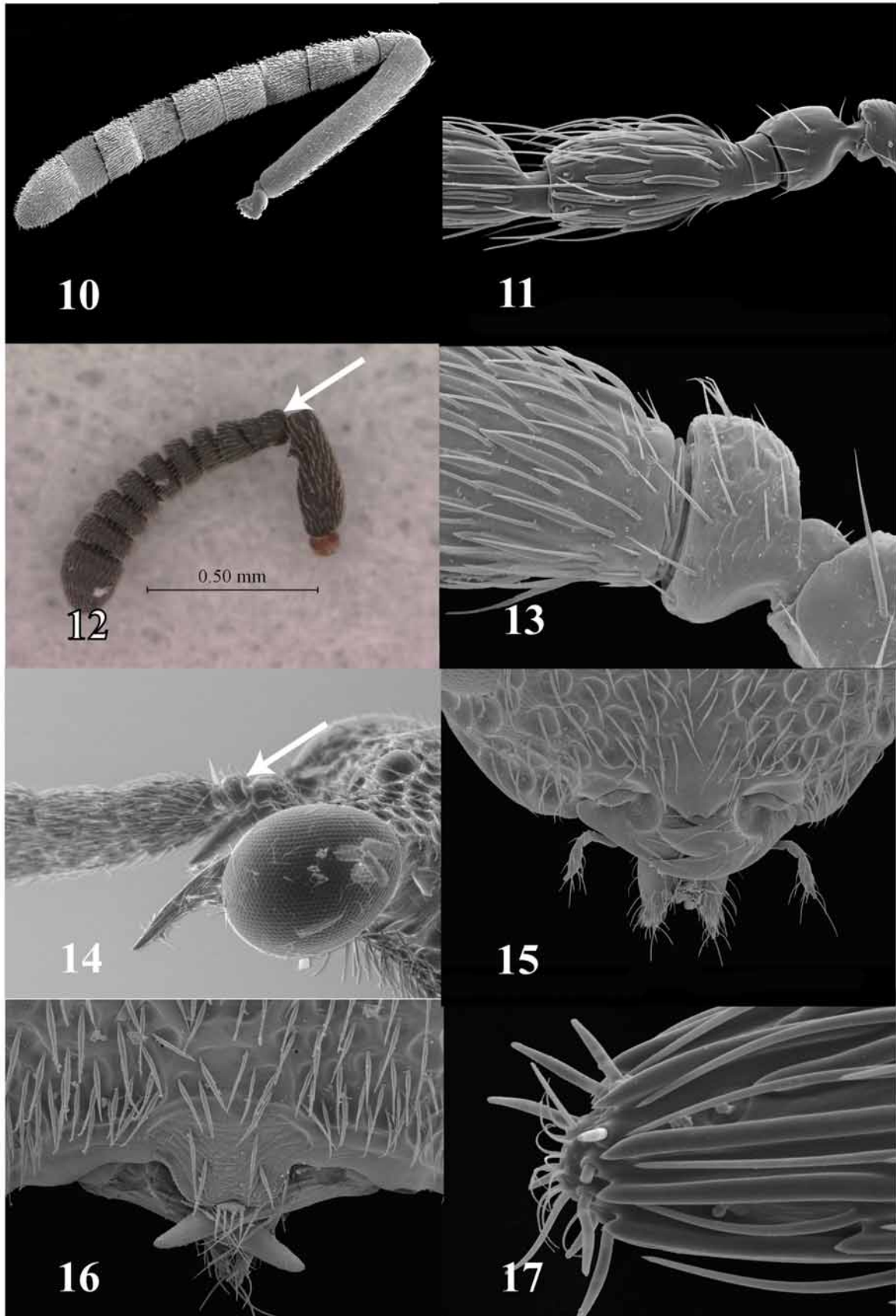
1, Present, horizontal, delimited by epicnemial carina (Fig. 26).

2, Present, sloping, delimited by epicnemial carina (Fig. 80).

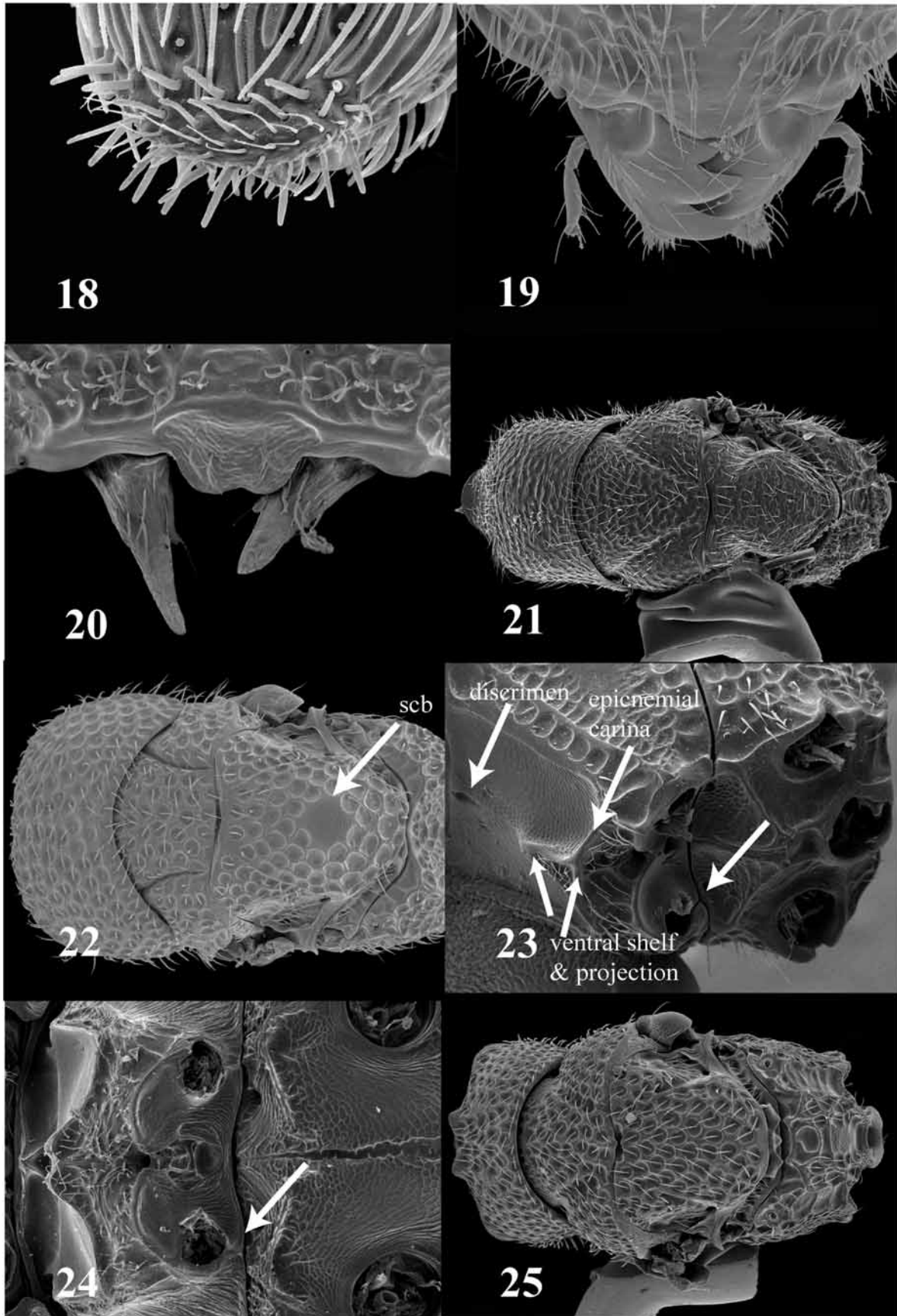
Lotfalizadeh *et al.* (2007) described this character and coded an additional state in which the mesopleural adscrobal carina delimits the ventral shelf anteriorly rather than the epicnemial carina. However, no taxa in this analysis display this state. The sloping ventral shelf supports *Philolema* and the lack of a shelf is seen primarily in taxa closer to the base of the hypothesized phylogeny (*Systole*, *Tetramesa*, *Macrorileya*, *Buresium*, *Bephratelloides*).



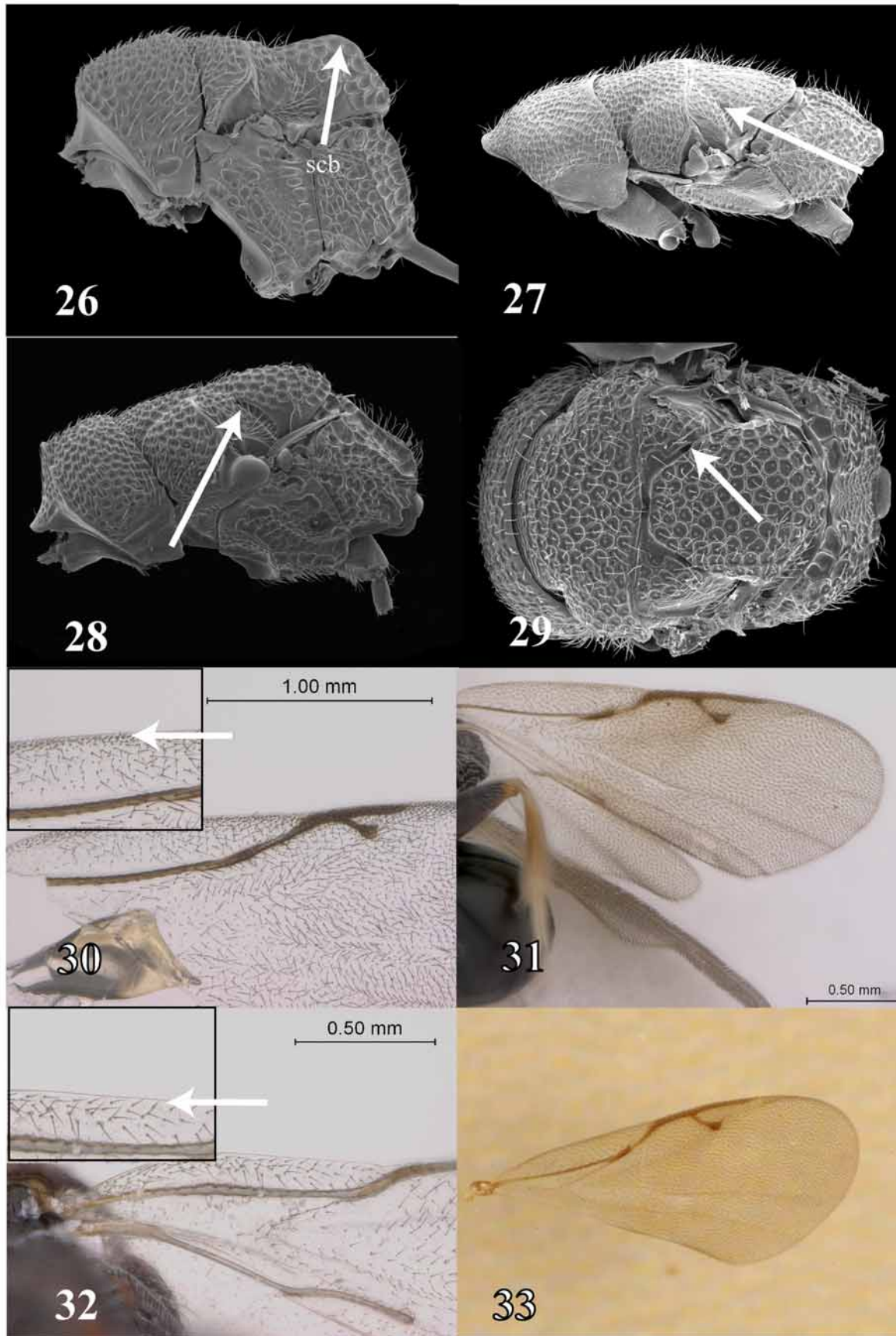
FIGURES 2–9. 2, *Macrorileyia oecanthi*, propodeum; 3, *K. erwini*, propodeum; 4, *K. lanceolatus*, posterolateral propodeum; 5, *Eurytoma bugbeei*, antenna; 6, *K. erwini*, antenna; 7, *K. erwini*, flagellomere close up; 8, *Systole albipennis*, antenna; 9, *Dirhinus n. sp.*, antenna. Note: all females.



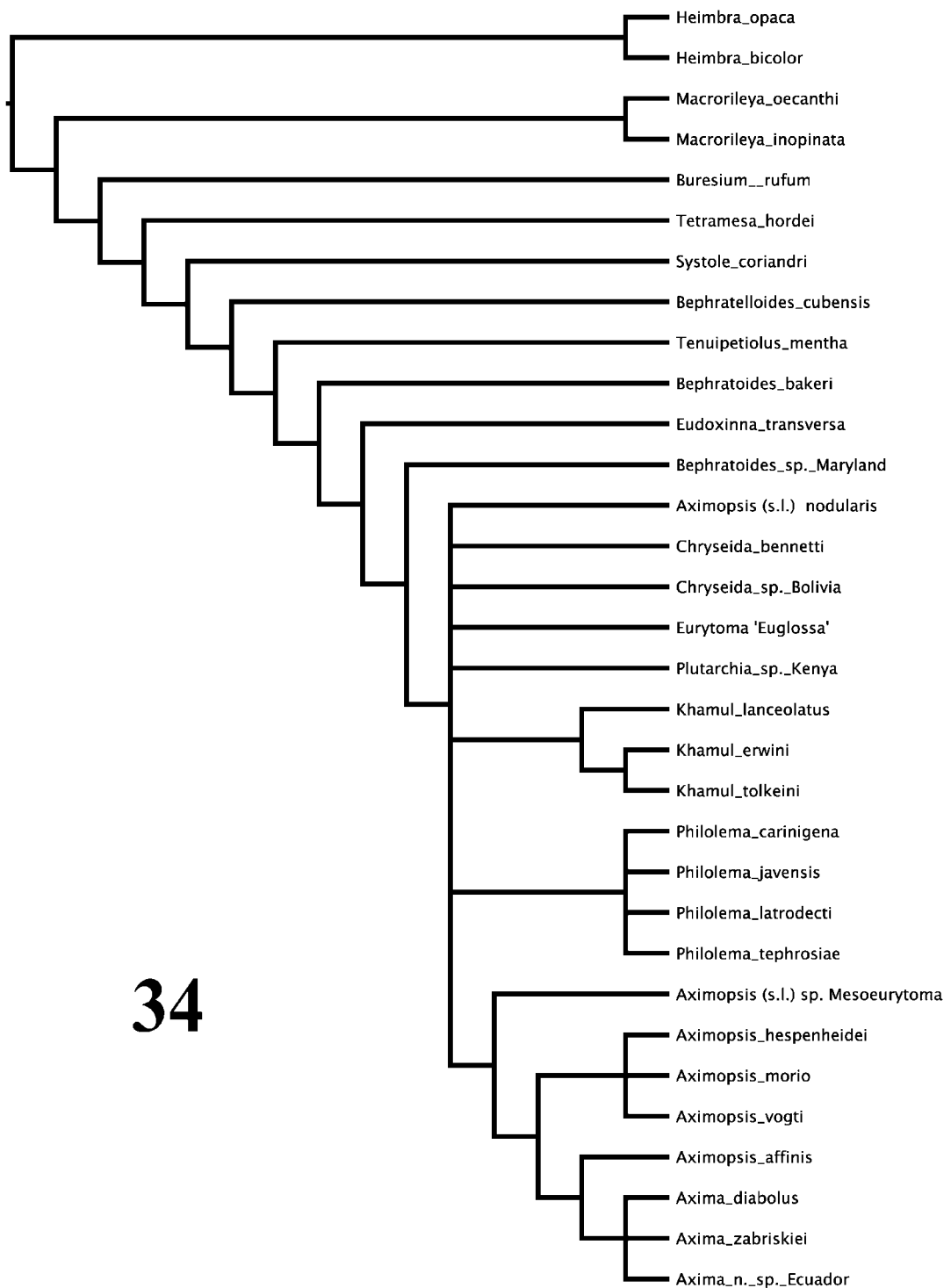
FIGURES 10–17. 10, *Conura* sp., antenna; 11, *Aximopsis vogti*, pedicel; 12, *Heimbra opaca*, antenna; 13, *K. erwini*, pedicel; 14, *Axima diabolus*, lateral head and basal antenna; 15, *K. erwini*, clypeus; 16, *K. lanceolatus*, clypeus; 17, *Eurytoma solenozopheriae*, apex clava. Note: all females.



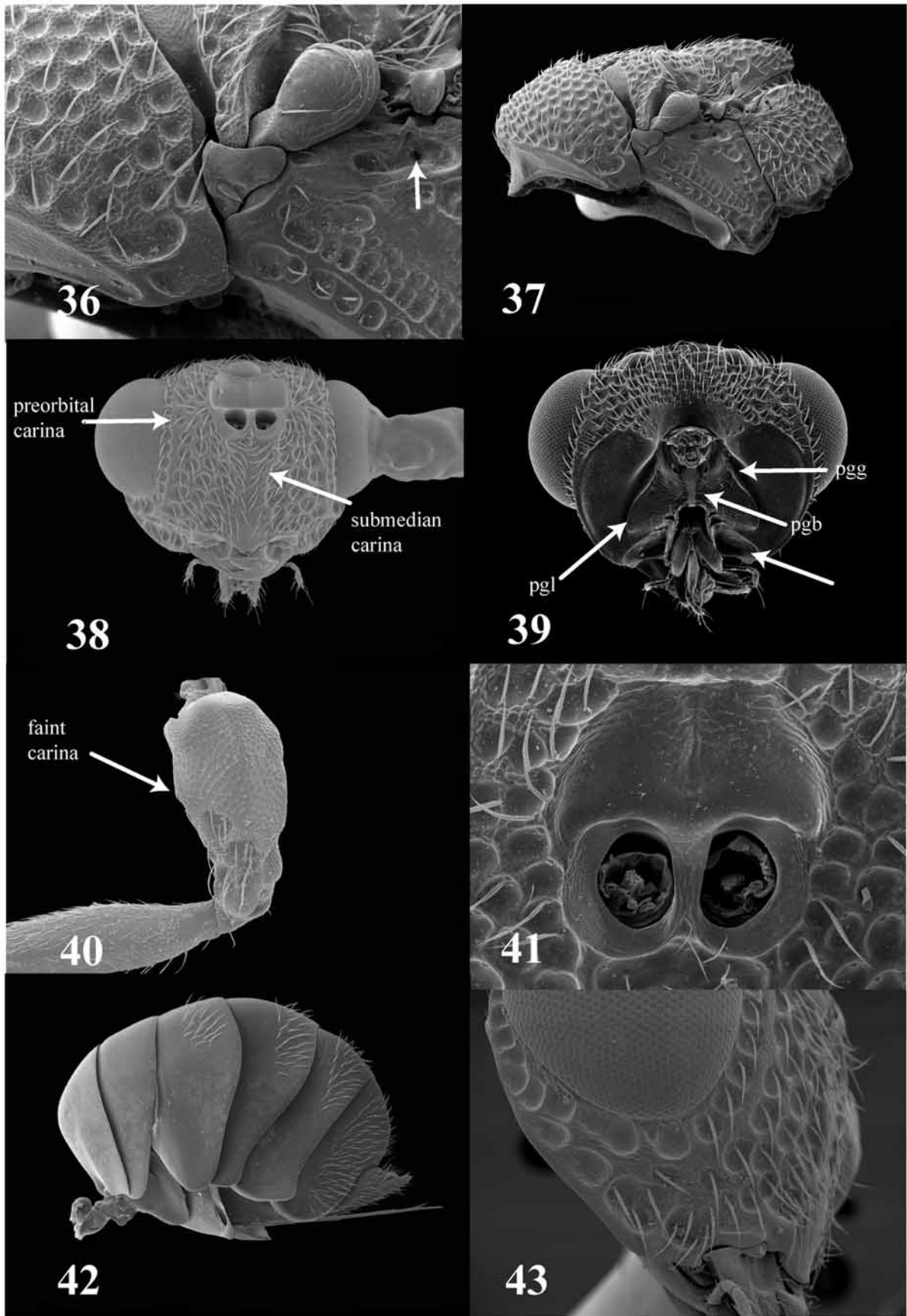
FIGURES 18–25. 18, *K. lanceolatus*, apex clava; 19, *K. erwini* (variant), mandibles; 20, *K. lanceolatus*, mandible; 21, *M. oecanthi*, dorsal mesosoma; 22, *K. erwini* (variant), dorsal mesosoma; 23, *K. erwini*, ventrolateral mesosoma; 24, *Bruchodape* sp., ventral mesosoma; 25, *A. vogti*, dorsal mesosoma. Note: all females.



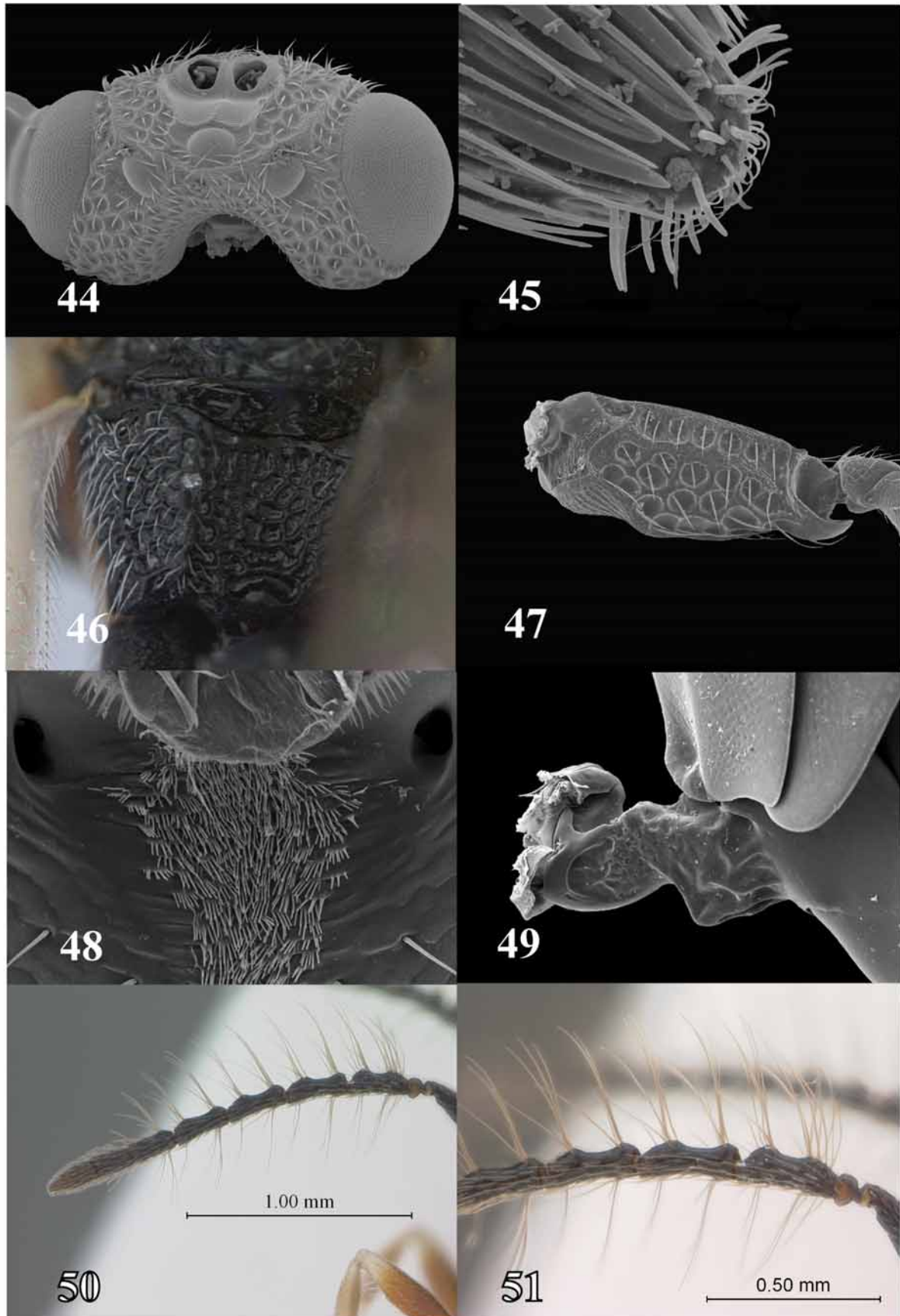
FIGURES 26–33. 26, *K. erwini* (variant), lateral mesosoma; 27, *Isosomodes* n. sp., lateral mesosoma; 28, *Philolema* sp., lateral mesosoma; 29, *Tenuipetiolus mentha*, dorsal mesosoma; 30, *K. lanceolatus*, ventral costal cell; 31, *K. gothmogi*, fore wing venation; 32, *Axima zabriskiei*, ventral costal cell; 33, *K. erwini*, fore wing. Note: all females.



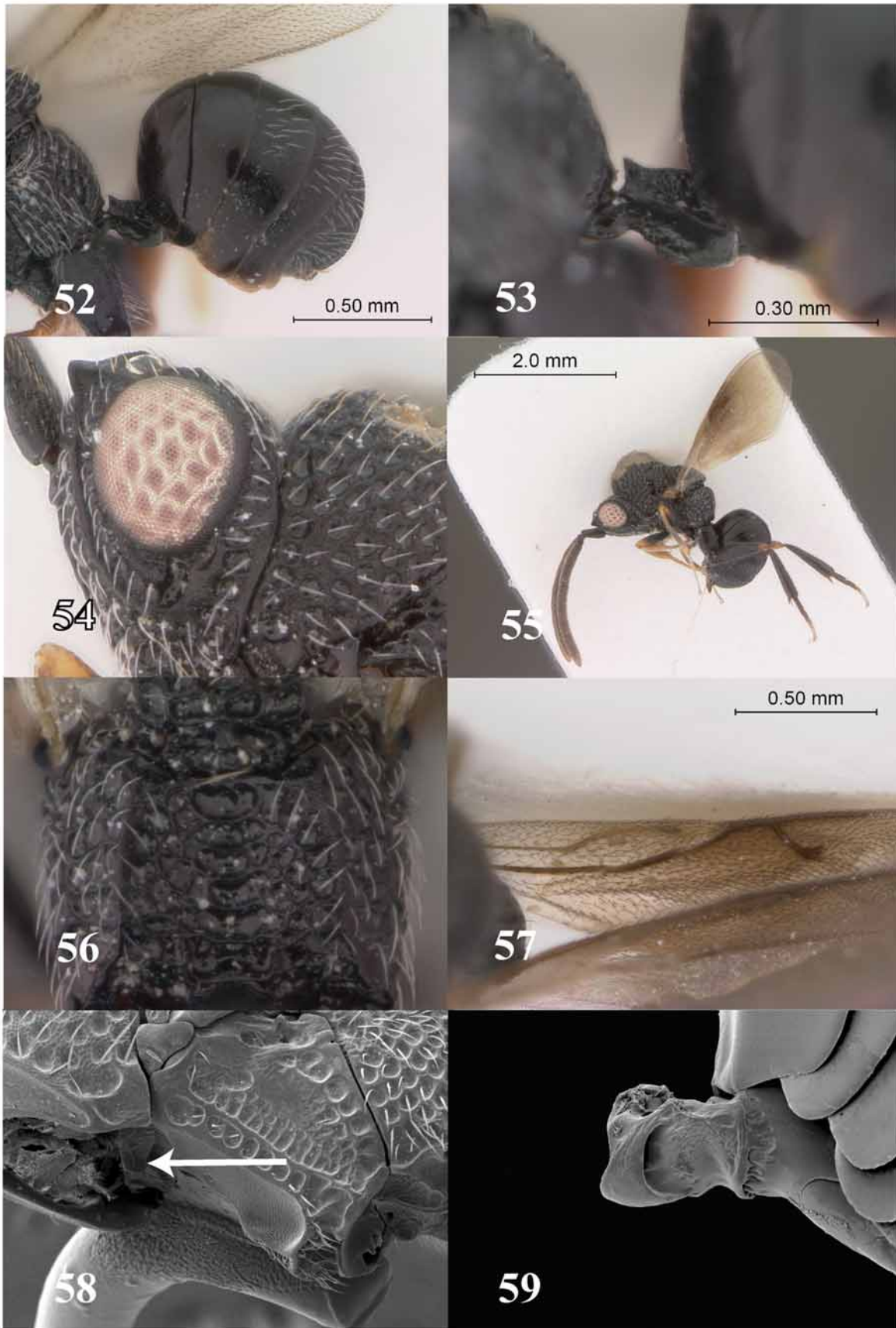
FIGURES 34. Strict consensus tree of 286 MPTs from unweighted analysis (step = 156; CI=0.53 ; RI=0.80).



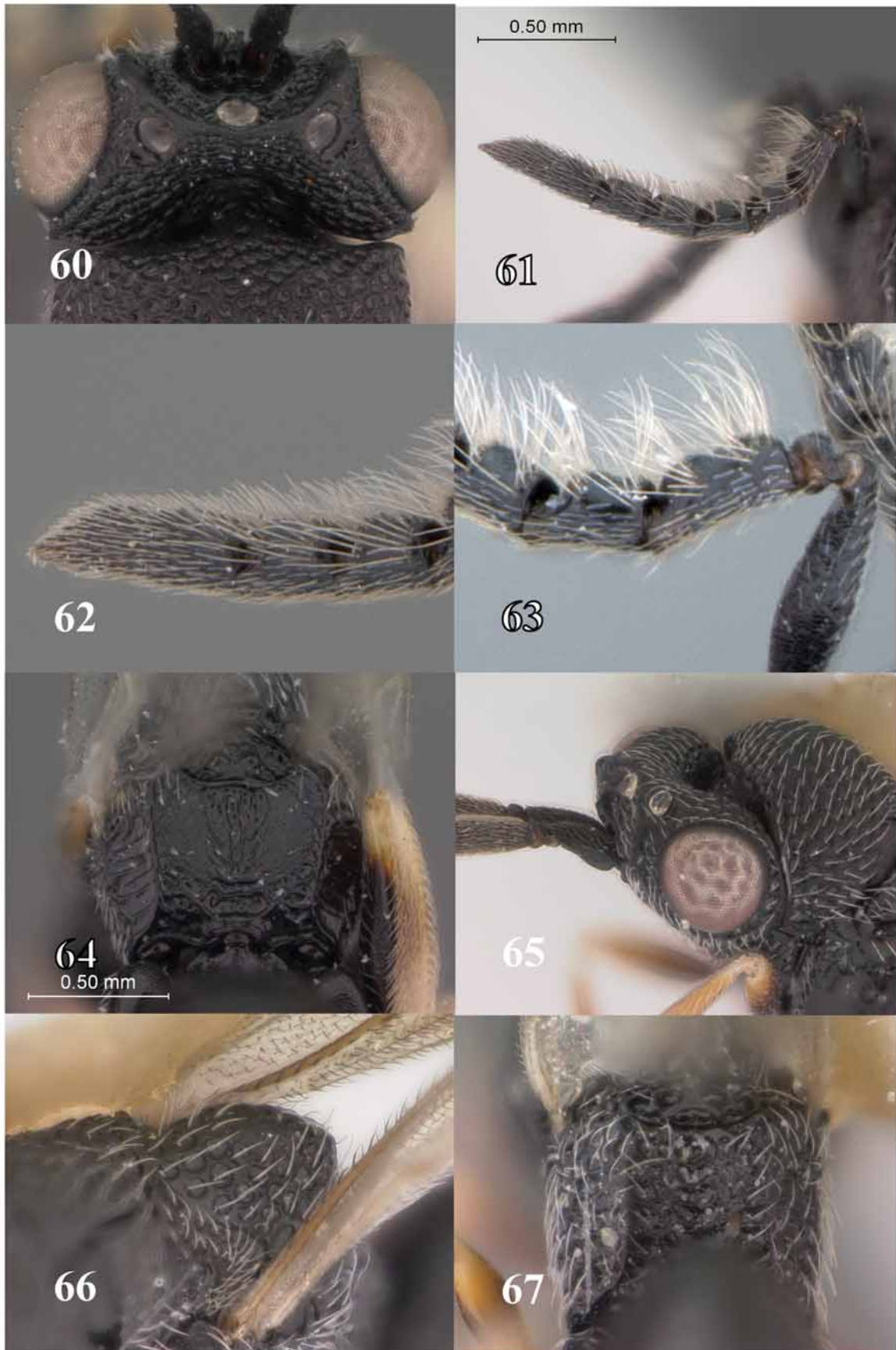
FIGURES 36–43. 36, *K. erwini*, lateral prepectus; 37, *K. erwini*, lateral mesosoma; 38, *K. erwini*, anterior head; 39, *K. erwini*, posterior head; 40, *K. erwini*, anterior fore leg; 41, *K. erwini*, scrobal depression; 42, *K. erwini*, lateral gaster; 43, *K. erwini*, malar space. Note: all females.



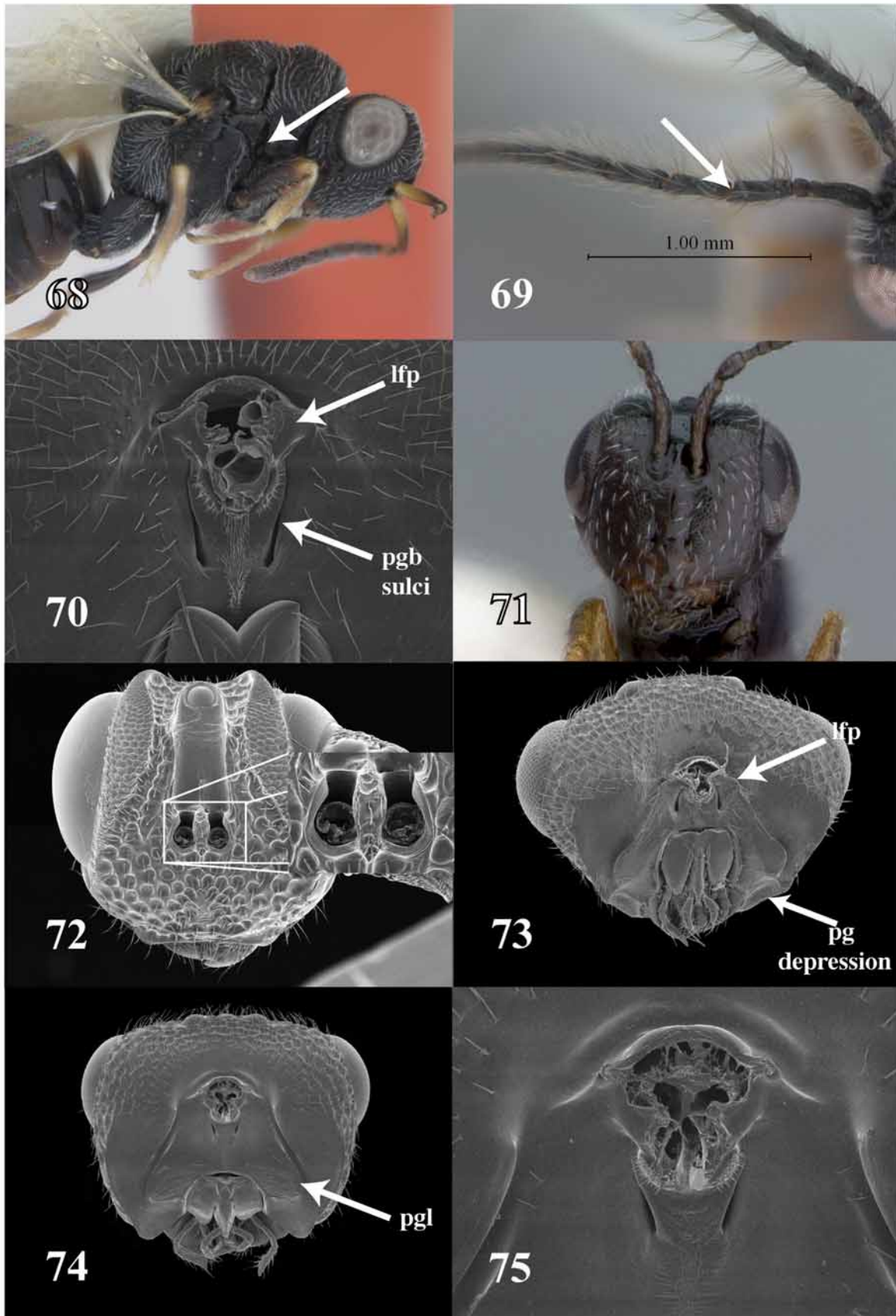
FIGURES 44–51. 44, *K. erwini*, dorsal head; 45, *K. erwini*, apex clava; 46, *K. erwini*, propodeum; 47, *K. erwini*, lateral procoxa; 48, *K. erwini*, digitiform ornamentation of postgenal bridge; 49, *K. erwini*, lateral petiole; 50, *K. erwini*, male antenna; 51, *K. erwini*, male antenna, pedicel to F4. Note: all females unless otherwise noted.



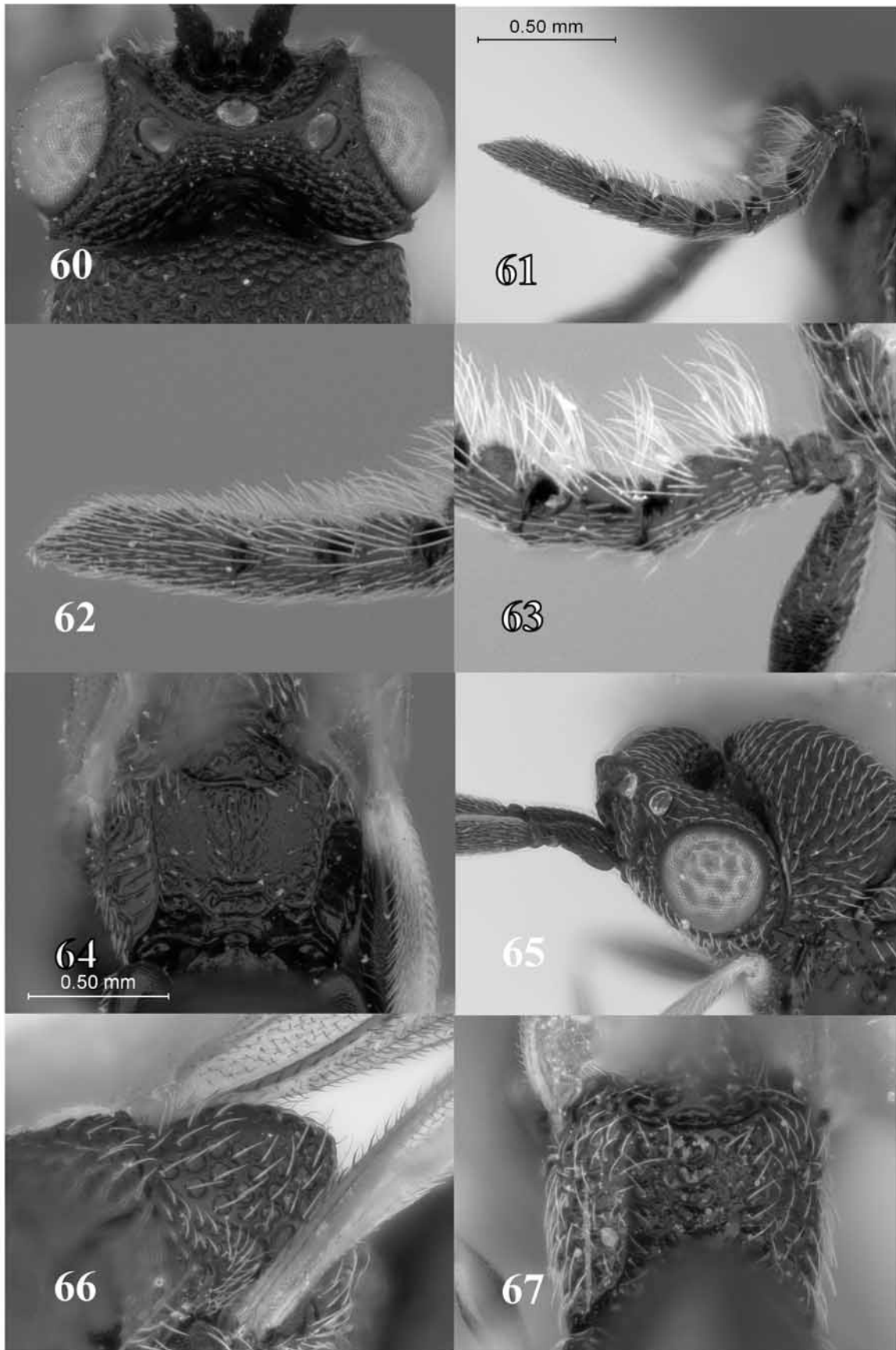
FIGURES 52–59. 52, *K. erwini*, lateral gaster; 53, *K. erwini*, lateral petiole; 54, *K. tolkeini*, lateral head; 55, *K. tolkeini*, lateral habitus; 56, *K. tolkeini*, propodeum; 57, *K. tolkeini*, fore wing venation; 58, *K. erwini*, lateroventral mesosoma; 59, *K. lanceolatus*, lateral petiole. Note: all females.



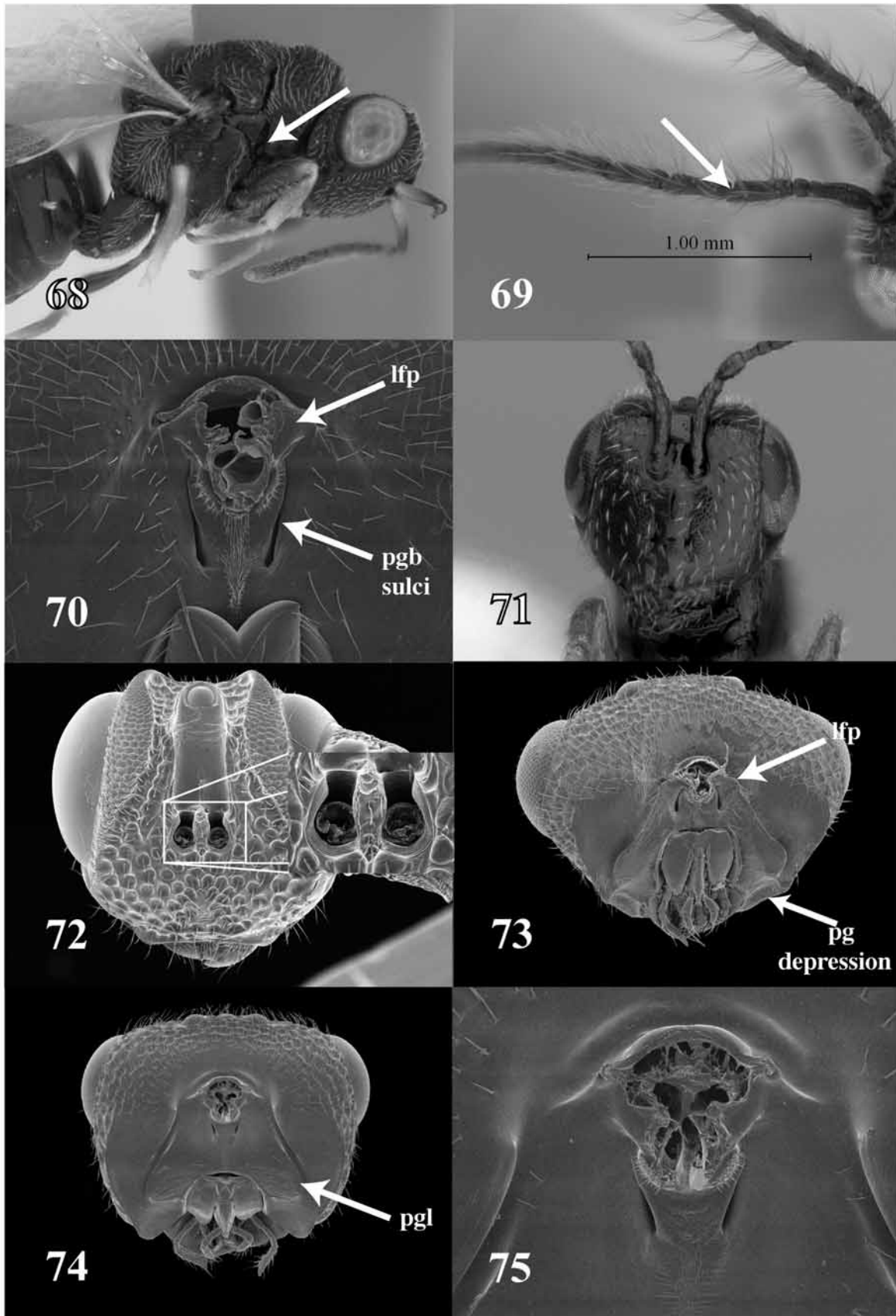
FIGURES 60–63. 60, *K. nr lanceolatus*, dorsal head; 61, *K. nr lanceolatus*, male antenna; 62, *K. nr lanceolatus*, male antenna, clava; 63, *K. nr lanceolatus*, male antenna, pedicel to F3; 64, *K. nr lanceolatus*, propodeum; 65, *K. gothmogi*, lateral head; 66, *K. gothmogi*, lateral scutellum; 67, *K. gothmogi*, propodeum. Note: all females unless otherwise noted.



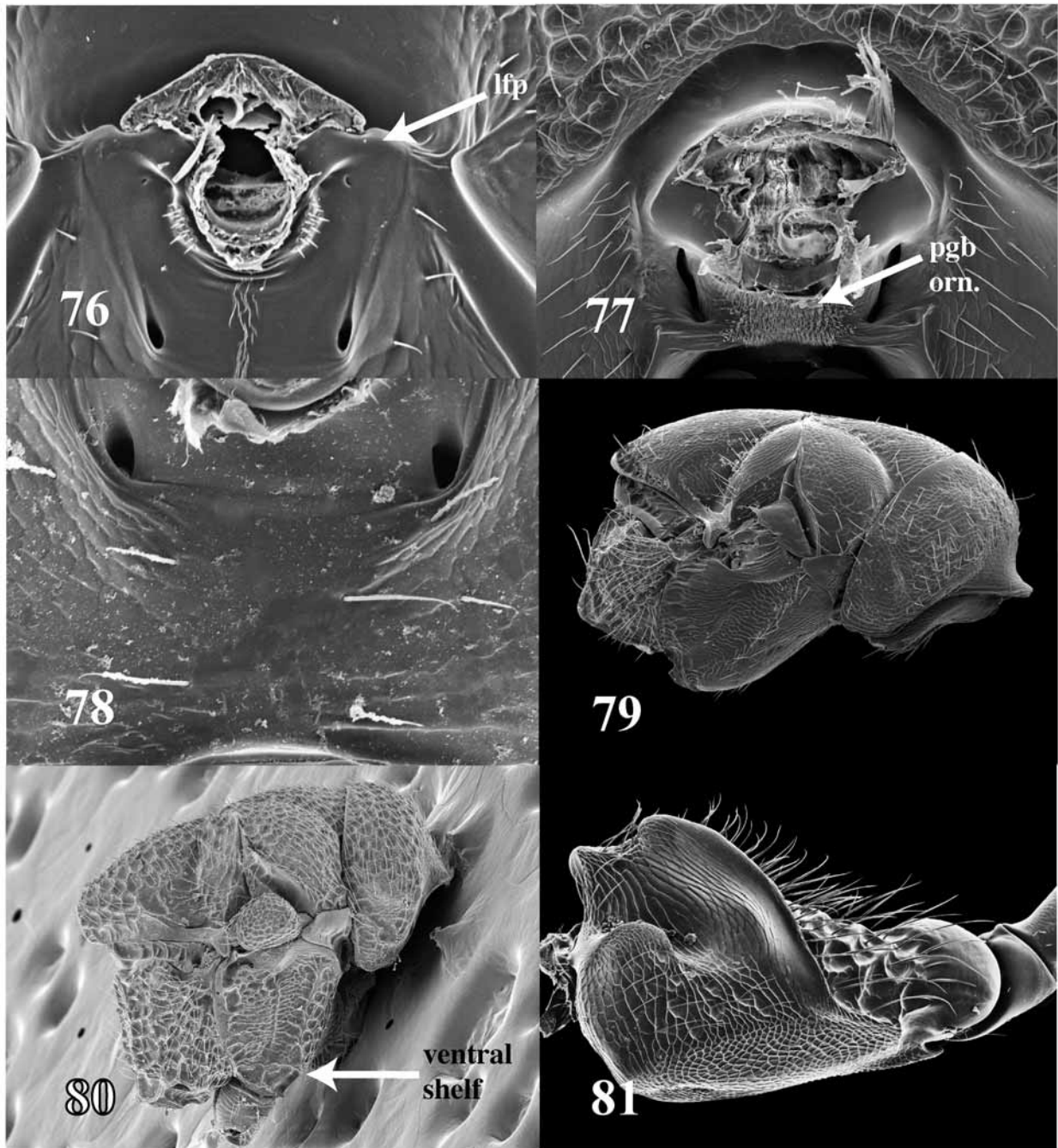
FIGURES 68–75. 68, *P. javensis*, lateral mesosoma; 69, *K. erwini*, male antenna, dorsal flagellomeres; 70, *M. oecanthi*, posterior head, postgenal bridge; 71, *M. oecanthi*, anterior head; 72, *Chryseida* sp. Bolivia, anterior head; 73, *P. latrodecti*, posterior head; 74, *Bephratelloides cubensis*, posterior head; 75, *B. cubensis*, posterior head, postgenal bridge. Note: all females unless otherwise noted.



FIGURES 60–63. 60, *K. nr lanceolatus*, dorsal head; 61, *K. nr lanceolatus*, male antenna; 62, *K. nr lanceolatus*, male antenna, clava; 63, *K. nr lanceolatus*, male antenna, pedicel to F3; 64, *K. nr lanceolatus*, propodeum; 65, *K. gothmogi*, lateral head; 66, *K. gothmogi*, lateral scutellum; 67, *K. gothmogi*, propodeum. Note: all females unless otherwise noted.



FIGURES 68–75. 68, *P. javensis*, lateral mesosoma; 69, *K. erwini*, male antenna, dorsal flagellomeres; 70, *M. oecanthi*, posterior head, postgenal bridge; 71, *M. oecanthi*, anterior head; 72, *Chryseida* sp. Bolivia, anterior head; 73, *P. latrodecti*, posterior head; 74, *Bephratelloides cubensis*, posterior head; 75, *B. cubensis*, posterior head, postgenal bridge. Note: all females unless otherwise noted.



FIGURES 76–81. 76, *Plutarchia* sp. Kenya, posterior head, postgenal bridge 77, *Heimbra opaca*, posterior head, postgenal bridge; 78, *Axima n. sp.* Ecuador, posterior head, postgenal bridge; 79, *Systole albipennis*, lateral mesosoma; 80, *P. latrodecti*, lateral mesosoma; 81, *Chryseida* sp. Bolivia, anterior procoxa. Note: all females.

69. Procoxa, sculpture:

0, Depression absent, evenly convex.

1, Depression present, not delimited ventrally by oblique carina.

2, Depression present, delimited ventrally by faint oblique carina (Figs. 40, 47).

3, Depression present, delimited ventrally by strong oblique carina (Fig. 81).

Khamul is the only taxon coded as state 1 and has a shallow depression delimited by a faint carina. The bulk of the taxa in this analysis were coded as state 3.

70. Procoxa, lateral areola:

- 0, Absent.
- 1, Elongate areola situated basolaterally in oblique groove (fig. 177).
- 2, Triangular areola situated basolaterally in oblique groove (fig. 180).
- 3, Elongate areola situated laterally on coxa.

This character was coded by Lotfalizadeh *et al.* (2007) and provides support for *Philolema s.l.* given that it has a unique lateral areola on the procoxa. *Khamul* completely lack and areola as do many of the taxa found closer to the base of the hypothesized phylogeny, while *Aximopsis s.l.* (excluding *nodularis* group) and *Plutarchia* code as state 2.

71. Body color:

- 0, Non-metallic
- 1, Metallic, usually blue or green

This character is autapomorphic in Eurytomidae, with the exception of some *metallica* species group (of *Bruchophagus s.l.* (Lotfalizadeh *et al.* 2007)), for species of *Chryseida*.

Results and discussion

The results presented herein largely agree with the hypotheses of relationship put forward by Lotfalizaedh *et al.* (2007) for Eurytominae in terms of taxon placement. For comparative purposes, I refer primarily to their Step 3 in analysis 1 results in which ‘consensus weighting’ was implemented to provide character weighting (fig. 3). The taxa spanning the basal nodes (*Macrorileya*, *Buresium*, *Tetramesa*, *Systole*) in this analysis correspond with those of the Lotfalizadeh *et al.* (2007) analyses. The same is also true of the taxa spanning the apical nodes (*Axima*, *Aximopsis*, *Philolema*) of the phylogenetic hypothesis presented herein, and it is in this area of the tree where *Khamul* is placed. Gérard Delvare was kind enough to code three species of *Khamul* (*erwini*, *tolkeini*, *lanceolatus*) into a modified matrix from one previously published (Lotfalizadeh *et al.* 2007) in order to ascertain its position relative to other eurytomine taxa (Delvare, unpublished data). In short, this reanalysis resulted in an apical *Aximopsis s.l.* clade that was rendered paraphyletic by *Chryseida* and *Axima* as follows: ((((((*Axima*+*Aximopsis s.l.*) +*Aximopsis s.l.*) +*Aximopsis s.l.*) +*Chryseida*) +*Aximopsis s.l.*) + (*Khamul*+*Eurytoma* San Alberto) + *Philippinoma*) + (*Eurytoma gyorfii*+*E. erythroaspis*)). Subtending this apical clade is a (*Bephratoides* spp. + *Eudoxinna* spp.) clade, which is in turn subtended by a grade of *Eurytoma* spp. Basad the aforementioned clades, is a sister clade containing *Philolema s.l.* (rendered paraphyletic by *Plutarchia bicariniventris*). Examining the cladograms presented by Lotfalizadeh *et al.* (2007; e.g. fig. 3), these aforementioned relationships are largely identical to previously published results (taking into account nomenclatural changes).

The results herein largely mirror, on a reduced scale, the apical relationships of *Axima* + *Aximopsis s.l.* and the placement of *Khamul*; however *Plutarchia* + *Philolema* is placed between *Axima* + *Aximopsis s.l.* and *Khamul* (Fig. 35). This is likely due to our restricted taxon sampling. The goals of delimiting the generic limits of *Khamul* and hypothesizing its phylogenetic placement were addressed and are illustrated in Figures 34 and 35. The successive reweighting analysis (Fig. 35) provided increased resolution for all of the outgroup and ingroup taxa, with a strongly supported (*Khamul lanceolatus* + (*K. erwini* + *K. tolkeini*)) relationship (Fig. 35). *Khamul* is supported as monophyletic by characters 52 (apex clava), 54 (notauli deep), and 56 (scutellar boss present). It would be placed in the *Philolema* genus group and likely in *Philolema s.l.* of Lotfalizadeh *et al.* (2007) as explained in the generic diagnosis below. However, the character support conflicts with the Palearctic distribution of *Philolema s.l.*

Khamul n. gen.

Type species: *Khamul erwini* Gates, by present designation.

Etymology: Named for the only Nazgl specifically named by J. R. R. Tolkein, Khaml, the Shadow of the East (aka Black Easterling) (Tolkein 1980). Gender masculine.

Diagnosis: Four apomorphies support the monophyly of *Khamul* as defined herein: flagellomeres cylindrical and tightly appressed, parallel-sided, with decumbent setation (female only; Figs. 6, 7), apex of clava with elongate sensillar region (Figs. 18, 45); deep notauli (Fig. 22); reticulate scutellar boss present (Figs. 22, 26). These are also shared with a taxon (*Eurytoma* San Alberto) coded by Lotfalizadeh *et al.* (2007). Globally, all but one of these characters is homoplastic (i.e., scutellar boss), a common occurrence in Eurytominae due to its mosaic evolutionary trends (Lotfalizadeh *et al.* 2007). The aforementioned characters may be used in combination with the following as a suite of characters for identifying *Khamul*: clypeus produced ventrally with apex broadly notched (Fig. 15), prepectus ~3/4 size of tegula (Figs. 36, 37), preorbital carinae continuous across vertex posterad anterior ocellus, pedicel roughly wedgelike in lateral view (Fig. 13) (also seen in *Eurytoma* San Alberto (Lotfalizadeh *et al.* 2007)), and infusate wing (Figs. 33, 55, 57). *Khamul* may be confused with the *Philolema* genus group (Lotfalizadeh *et al.* 2007) with which it shares a depressed postgena at the oral fossa (Fig. 39), the postgenal lamella (PGL) smoothly joining the posterior margin of the gena (Fig. 39), and the supraclypeal area bound by two submedian carinae (Fig. 38), but it can be reliably separated by the aforementioned diagnostics. It may also be confused with *Aximopsis s.l.* given that *Aximopsis s.l.* shares many characters with *Philolema s.l.* (Lotfalizadeh *et al.* 2007): deep sublateral prepectal pit (Fig. 68), mesopleuron with a long sloping ventral shelf (horizontal in *Aximopsis s.l.*) (Fig. 80), ventral shelf medially projecting (Fig. 23), subalar pit deep (Fig. 36), procoxa with oblique carina delimiting basal reticulate depression (receives venter of head) (Figs. 40, 47), and lateral and anteroapical surface umbilicate punctate. *Khamul* possesses a small sublateral prepectal pit, but it is usually not visible in lateral view due to the closely approximated pronotum and mesopleuron. This close approximation is typically not observed in other taxa sharing the pit (e.g., *Philolema s.l.*, *Axima*, *Chryseida*, *Aximopsis s.l.*) because the prepectus is longer. The other characters seen in *Philolema s.l.* (ITS not dorsally produced and flat LFP, both homoplastic; see character descriptions), more useful for separating it from *Aximopsis s.l.*, are absent in *Khamul*. *Khamul* has the ITS not produced, the LFP convex, and a simple change of sculpture and a slight angulation along the track on which the procoxal carina occurs in *Philolema s.l.*, *Axima*, *Chryseida*, and *Aximopsis s.l.*

In the key to eurytomid genera of Burks (1971), *Khamul* runs to couplet 25 whereupon it splits the diagnostic characters. In the first half of the couplet, *Khamul* possesses a reduced prepectus, smaller than the tegula, and has the epicnemium impressed to receive the procoxae; however, the antennae are sexually dimorphic and have only 10 segments in the female (if the fused clava is counted as one, 12 if not) and 11 in the male. Proceeding through the second half of the couplet, ignoring the prepectal character, couplet 43 is ultimately reached where *Bephratelloides* and the *Eurytoma* complex key. *Khamul* has six funiculars, a solid clava, and infusate fore wing much like *Bephratelloides*, but differs in that *Khamul* has a smaller prepectus, black coloration, preorbital carina, scutellar boss, and cylindrical antenna. *Bephratelloides* has a large, triangular prepectus, largely golden/orange coloration, no preorbital carina or scutellar boss, and non-cylindrical antenna.

Description. Female. Length 3.3–5.3 mm. Head, body, and coxae black, non-metallic. Scape black; pedicel mostly black, especially basally, often dark brown apically; flagellum dark brown to blackish. Tegula pale brown or black. Pronotum brown on anterolateral panel. Legs and pretarsus brown, except extreme apices of femora, tibiae, and tarsomeres whitish, generally darker basally and lightening apically (Fig. 1). Sculpture generally umbilicate with interstices alveolate (Figs. 1, 22, 26, 37).

Head (Figs. 1, 15, 16, 19, 20, 38, 39, 41, 43, 44, 48, 54, 60, 65). Umbilicately punctate dorsally, laterally, and anteriorly, 1.40–1.43X as broad as high. Lower tentorial pits small; two submedian carinae extending ventrally from toruli and connecting with smooth supraclypeal area (Fig. 38); genal carina present, eye 1.8–3.4X

as high as malar space (Figs. 38, 54); scrobal depression carinate laterally, carina usually distinct dorsally (Fig. 41), depression minutely elevated medially in dorsal half (Fig. 41); mandible with lower and middle teeth acute, upper tooth rounded; clypeus produced ventrally, apical margin broadly emarginate (Figs. 15, 16); preorbital carinae present, extending medially between anterior and lateral ocellus to meet posterad anterior ocellus (Figs. 38, 65). Posterior surface of head with postgenal lamina, postgenal grooves evidently ridged, divergent ventrally, extending beyond upper margin of hypostomal bridge; dorsal margin of lateral foraminal plate visible, convex; postgenal sulci vestigial; postgenal depression present ventrally between hypostomal fossa and genal carina; postgenal bridge ornamented with digitiform expansions (Fig. 48). *Antenna* (Figs. 6, 7). Scape reaching dorsal margin of anterior ocellus. Pedicel wedge-shaped in lateral view, with strong basal bottle-neck, narrowed ventrally; anellus very thin, closely appressed to F1 (Fig. 13); F1–6 cylindrical, tightly appressed, parallel-sided, each F with multiple rows of multiporous plate sensilla and dense, decumbent setation; claval segments fused, apex with elongate sensillar area (Figs. 18, 45).

Mesosoma (Figs. 1, 22, 23, 26, 36, 37, 46, 56, 66, 67). Pronotum 1.74–2.0X as broad as long. Mesoscutal midlobe 0.75–1.27X as broad as long; notauli complete, narrow and deep (Fig. 22) (except not deeply impressed in *K. lanceolatus*). Lateral lobe of mesoscutum finely reticulate in anterior half, separated by step-like ridge from umbilicately punctate posterior half (Fig. 37). Scutellum 0.67–0.72X as broad as long at its widest; broadly convex dorsally, with scutellar boss dorsomedially (Figs. 22, 66). Dorsellum glabrous except for anterolateral row of setae (Figs. 3, 4, 56). Lateral panel of propodeum and callus umbilicately punctate, separated from median area by carinae (Fig. 3, 4, 46), carinae bordered medially by row of umbilicate punctae, median channel formed by irregular foveae bordered by smaller, shallower punctae (Fig. 3, 4, 46), propodeal angle relative to longitudinal axis mesosoma >90 but <130 ; lateral prepectus triangular, broadly rounded apically, smooth; sublateral prepectal concavity present, obscured by appressed mesopleuron and pronotum; ventral prepectus with median flange (Fig. 58), depressed along posterior margin (Fig. 23); epicnemium flattened, with superficial submedial, shallow depressions to receive procoxae (Fig. 23), discrimen visible as anteromedial ovate depression, in anteroventral view with ventral shelf bearing a projection inserted between apices of procoxae (Fig. 23); mesopleural shelf horizontal. Procoxa slightly depressed anteriorly, anterobasally and posteriorly reticulate (Figs. 40, 47), anteroventrally and laterally umbilicately punctate (Fig. 47). Mesocoxa glabrate to finely reticulate; mesocoxal foramina narrowly open posteriorly (Fig. 23). Forewing (Figs. 33, 53, 55) usually infuscate at least along anterior margin (Figs. 33, 55, 57), venation brown, setae on disk dark, absent in basal 1/3 except for basal setal line and cubital setal line, basal cell with 2–3 setae near apex (Figs. 30, 31, 33); postmarginal vein ranging from 1.4–2.7X length marginal vein and stigmal 0.70–2.4X length of marginal vein.

Metasoma (Figs. 1, 42). Petiole 3.0–4.0X as broad as long in dorsal view, some fine sculpturing laterally and ventrally, glabrous; anterior transverse carina protruberant laterally, paired submedian carinae ventrally define triangular fovea (except see *K. lanceolatus* description) (Figs. 49, 59). Gaster ovate in lateral view, slightly acuminate posteriorly; all terga with some effaced reticulation, increasingly defined posteriorly, asetose along midline; Gt1 with paired depressions dorsad petiole, line of three+ setae dorsolaterally in posterior half (Figs. 42, 49); Gt3–4 setose dorsolaterally in posterior half; Gt5 nearly entirely setose; syntergum completely setose.

Male. Similar to female in coloration and structure except as follows: five funicular segments and a two-segmented clava (Figs. 50, 61); funiculars pedicellate with whorls of setae on dorsal surface basally and apically, except F5 with strong basal whorl only; and apex of each funicular body angled (Figs. 63, 69). Petiole roughly as broad as long in dorsal view, with anterodorsal margin carinate (Fig. 53) dorsolateral margin finely carinate.

Key to species of *Khamul*

- 1 Tegula golden or brownish2
1' Tegula black (Fig. 65).....*Khamul gothmogi*, n. sp.
2 Mandible with lower tooth as an equilateral triangle, curved (Fig. 19).....3
2' Mandible with lower tooth as an isosceles triangle, linear (Fig. 20)..... *Khamul lanceolatus*, n. sp.
3 Preorbital carina produced as blunt, triangular process between lateral ocellus and eye (Fig. 54); distinct reniform subocular fovea present (Fig. 54); hind tibia black (Fig. 55) *Khamul tolkeini*, n. sp.
3' Preorbital carina not produced (Figs. 38, 44); subocular fovea absent (Fig. 43); hind tibia yellow to pale brown (Fig. 1).....*Khamul erwini*, n. sp.

Khamul erwini Gates, n. sp.

(Figs. 3, 6, 7, 13, 15, 19, 22, 23, 26, 33, 36–53, 69)

Etymology: *erwini* (Latinized, noun) = genitive singular, masculine, named in honor of Terry Erwin for his groundbreaking canopy fogging efforts.

Diagnosis and identification: Tegula brownish, apical mandibular tooth as an equilateral triangular and curved, both characters are shared with other species of *Khamul* except *K. gothmogi* (black tegula) and *K. lanceolatus* (linear mandibular tooth). Preorbital carina finely produced ventrally, not delimiting a reniform subocular fovea (Fig. 43); carina not produced as a triangular process between lateral ocellus and eye.

Description: Female holotype. Length 3.4 mm. Head, body, and coxae black. Scape black; pedicel black basally, dark brown apically; flagellum dark brown. Tegula pale brown. Pronotum brown on anterolateral panel. Legs and pretarsus brown, except extreme apices of femora, tibiae, and tarsomeres whitish. Wings lightly infuscate, darker anteriorly, wing veins brown.

Head. 1.4X as broad as high; 1.2X wider than pronotum; HTE:msp 2.07. POL 5.0X as long as OOL. Width of oral fossa 0.44X width of head. Preorbital carina of uniform width beneath eye, reniform subocular fovea absent, carina not produced as triangular tooth at vertex. Scape 3.33X as long as broad. Antennal segment relative measurements 35:7:1:30:23:20:20:21:19:30. Clava 2.31X as long as broad.

Mesosoma. Dorsal pronotum 1.84X as broad as long. Mesoscutal midlobe 1.27X as broad as long. Scutellum 0.72X as broad as long; broadly convex dorsally, scutellar boss present, subequal in dimensions to adjacent umbilicate puncta and surrounding border combined. Dorsellum disc composed of a central -shaped structure connected laterally to submedian carinae (Fig. 46). Propodeal median channel composed of transverse reniform punctae, channel bordered laterally by smaller punctae and irregular rugosity (Fig. 46). Relative measurements marginal:postmarginal:stigmatal veins as 27:40:20; stigmal vein evenly arcuate (Fig. 33); infuscation not reaching disc margins.

Metasoma. Petiole 3.0X as broad as long in dorsal view; fine transverse carina anteriorly, protruberant laterally; bicarinate ventrally, defining triangular fovea, produced in lateral view (Fig. 49). Gastral terga measurements in dorsal view on median line as 16:20:38:34:20:6; syntergum not visible in dorsal view (Fig. 42).

Male. Similar to female except as follows: Funicle 5-segmented (Figs. 50, 51), inconspicuously pedicellate, each funicular with two whorls of setae and asymmetrically produced apically with circular carina, carina maximally produced lateroventrally (Fig. 69), thus each pedicel obscured; scape 2.92X as long as broad. Antennal segment relative measurements 35:6:1:33:31:29:28:23:47. Clava 4.27X as long as broad. Petiole reticulate dorsally, 1.53X as broad as long in dorsal view; carinate flange present anterodorsally; dorsal lateral carinae strong, incomplete anteriorly; dorsal median carina present in posterior 2/3; convex ventrally in lateral view (Figs. 52, 53). Gastral terga measurements in dorsal view on median line as 19:30:37:40:25:9, syntergum not visible in dorsal view.

Variation. Coloration on the femora of both sexes ranges from orange brown to brown to dark brownish black, with the apices grading from the predominant color basally through a brownish yellow to pale yellow or whitish. One male with median channel somewhat more well defined anteriorly, scutellum convex at boss, and stigmal vein straight.

Type material (19♀ 3♂; held in trust at USNM). Holotype ♀; ECUADOR: Orellana: Tiputini Biodiversity Station, 216m, 0037°55'S 76°08'39"W, 8.ii.1999, Lot 2020, Trans. 3, T. Erwin et al. Canopy fogging bare leaves, some w/ bryophytic/lichenous coat; Restrictions Apply NMNH-DCB/EPN, Agreement 39. Paratypes 18♀ 3♂ (all held in trust at USNM); same data as holotype, dates differing as follows: 8.ii.1999, Lot 2028, Trans. 3 (2♀); 8.ii.1999, Lot 2022, Trans. 3 (1♀); 8.ii.1999, Lot 2021, Trans. 3 (2♀); 8.ii.1999, Lot 2020, Trans. 3 (1♀ 1♂); 8.ii.1999, Lot 2039, Trans. 4 (1♂); 30.vi.1998, Lot 1820, Trans. 3 (1♀); 5.ii.1999, Lot 2088, Trans. 9 (1♀ 1♂); 5.ii.1999, Lot 2086, Trans. 9 (4♀); 8.ii.1999, Lot 2024, Trans. 3 (1♀); 5.ii.1999, Lot 2085, Trans. 3 (1♀); 21.x.1998, Lot 1997, Trans. 10 (1♀); 6.ii.1999, Lot 2066, Trans. 7 (1♀); 5.ii.1999, Lot 2087, Trans. 9 (1♀); 5.ii.1999, Lot 2088, Trans. 9 (1♀).

Discussion. The male included in the type series most closely matches the diagnostic characteristics of the females of the type series. Several additional specimens, of both sexes that are similar to *K. erwini* are discussed below as variants and cannot be definitively placed at this time. These specimens sometimes originate from a different geographic area. The sample including the variant specimens may be insufficient to fully explore the morphological variation and to determine whether they are conspecific or represent distinct species. Additional material, especially reared, would provide the means to solve some of these issues.

Material examined. COSTA RICA: Puntarenas: R. B. Carara, Est. Quebrada Bonita, 50m, iii.1994, R. Guzmán, L_N_194500_469850, #2803; COSTA RICA INBIOCRI001752495 (1♀ INBio); Puntarenas: Res. Biol. Carara, Est. Carara, 200m, ii.1990, R. Zuniga, L_N_195250_478700; COSTA RICA INBIOCRI000645008 (1♀ INBio); Puntarenas: Golfito, Sendero a Sirena, 100m, 05.v.2001, J. Azofiefa.Libre, L_S_276500_514200, #63265; INB0003333425 (♂), INB0003333429 (♂), INB0003333433 (♂), INB0003333427 (♀), (1♀ 3♂; INBio); Puntarenas: Est. Agujas, 300m, 9–25.ii.2001, J. Azofiefa.Libre, L_S_276750_526550, #62901; INB0003318596 (1♀ INBio); Heredia: La Selva Biol. Station, 3km S. Puerto Viejo, 10 26°N 84 01'W; 16.vii.1992, H. A. Hespenheide (1♀ USNM); Guanacaste: Arenales, W. side Volcán Cacao, 900m, xi–xii.1990 (1♀ MZCR); Puntarenas: Golfo Dulce, 24km W. Piedras Blancas, 200m, vi–viii.1989, P. Hanson (1♀ MZCR); Puntarenas: PN Corcovado, Est. Sirena, 50m, iv–viii.1989 (1♀ MZCR).

The material from Costa Rica differs from nominate *K. erwini* primarily by the presence of the humplike scutellum in lateral view. Other characters vary as in *K. erwini*, namely the extent of the infuscation on the fore wing, coloration of the legs, and eye color ranging from pinkish to red. The specimen from Est. Carara has a disfigured metapleural/propodeal region with the left metapleuron stretched to the midline of the petiole, normally occupied by propodeum. The dorsellum is expanded posterolaterally, extended toward the petiole and contacting the expanded left metapleuron. The propodeum midline is offset by this and oriented at 45 toward the right metapleuron.

BRAZIL: Linhares, E. Santo, ix.72, ♂. Alvarenga (1♀ 2♂; labeled as *Khamul* variant 1; CNCI). The female differs from *K. erwini* by a brown flagellum (as in *K. gothmogi*), dense effaced reticulation on Gt1 (usually smooth in *K. erwini*), scutellum slightly convex in lateral view. The two males possess distinctly pedicellate funiculars (except F4) that lack the apicoventral angulate flanges subtending each pedicel apically (cf. Fig. 50), the propodeum has a better developed median channel (cf. Fig. 54).

COLOMBIA: Amazonas: PNN Amacayacu, Matamata, 300m, San Martn, 323°01'N 70°06'01'W, 26.v–6.vi.2000, A. Parente, #680 (1♂; labeled as *Khamul* variant 2; USNM). Same as ♂, but 150m, 19–26.iii.2000, B. Amado, ♂.82 (1♀; labeled as *Khamul* variant 2; IAVH). Same as for ♀, but 22–30.v.2000, B. Amado, #90 (1♀; labeled as *Khamul* variant 2; IAVH). The male has a distinct median carina dorsally on the petiole and the claval segments are longer than in males of the type series. Females have the flagellum more brownish and the petiole is slightly longer than in the type material.

ECUADOR: Napo: Reserva Etnica Waorani, Transect Ent., 1km S. Okone Gare Camp, 0039'10"S 76°26'00"W, 220m, 2.vii.1995, T. Erwin et al. Canopy fogging, Lot # 1090, t6..10, terre firme forest; Restrictions Apply NMNH-DCB/EPN, Agreement 39 (1♂; labeled as *Khamul* variant 3; held in trust at USNM). This male does not possess the apical asymmetrical expansion of the male paratype; further, its two claval segments are distinctly separated. The median channel of the propodeum is deep and well defined. The scutellum in lateral view is convex as opposed to flat. A second male is very similar to the variant 3 male but has the scutellar boss covering 2/3 the dorsal surface and the stigmal vein straight.

***Khamul gothmogi* Gates, n. sp.**

(Figs. 31, 65–67)

Etymology: *gothmogi* (Latinized, noun) = genitive singular, masculine, named in honor of Gothmog, Lord of the Balrogs, High Captain of Angband (Tolkein 1977).

Diagnosis and identification: Tegula black, apical mandibular tooth as an equilateral triangular and curved. Preorbital carina is finely produced ventrally but does not delimit a reniform subocular fovea; carinae expanded into a rounded process between lateral ocellus and eye (Fig. 65). Scutellum convex in lateral view (Fig. 66) as opposed flat in *K. erwini* (Fig. 37). Propodeal median channel is distinctly delimited, particularly anteriorly (Fig. 67).

Description: Female holotype. Length 3.3 mm. Head, scape, tegula, body, coxae, and basal 7/8 metafemur black. Basal third pedicel, flagellum, and basal 2/3 pro- and mesofemur brown. Apices femora, tibiae, tarsi pale golden. Pretarsus brown. Fore wing infuscate, venation brown.

Head. 1.41X as broad as high; 1.1X wider than pronotum; HTE:msp 2.0. POL 3.0X as long as OOL. Width of oral fossa 0.40X width of head. Clypeus not separated from supraclypeal area by carina. Preorbital carina of uniform width beneath eye, reniform subocular fovea absent, carina produced as blunt lobe at vertex. Scape 3.33X as long as broad. Antennal segment relative measurements 34:6:1:35:25:26:23:22:20:35. Clava 2.33X as long as broad.

Mesosoma. Dorsal pronotum 2.0X as broad as long. Mesoscutal midlobe approximately as broad as long. Scutellum 0.67X as broad as long; broadly convex dorsally, scutellar boss present, subequal in dimensions to three adjacent umbilicate punctae and surrounding border combined, distinctly convex in lateral view (Fig. 66). Dorsellum disc composed of a central -shaped structure, depressed dorsally, connected laterally to submedian carinae (cf. Fig. 64); posterior invagination entire. Propodeal median channel distinct, delimited laterally by carinae, composed of rectangular foveae (Fig. 67), channel bordered laterally by numerous smaller punctae. Relative measurements marginal:postmarginal:stigmal veins as 21:37:33; stigmal vein arcuate.

Metasoma. Petiole 3.0X as broad as long in dorsal view; fine transverse carina anteriorly, protruberant laterally; bicarinate ventrally, defining triangular fovea, produced in lateral view. Gastral terga measurements in dorsal view on median line as 20:30:33:23:15:6, syntergum not visible in dorsal view.

Male. Unknown.

Variation. The paratype from Waorani has a stigmal vein that is slightly bent (angulate) rather than smoothly arcuate. Also, the preorbital protuberance of the specimen is slightly smaller and narrower than that of the holotype. The area occupied by the scutellar boss also is slightly variable among members of the type series, ranging from 1–3 foveal equivalents.

Type material (3♀, held in trust at USNM). Holotype ♀; ECUADOR: Orellana: Tiputini Biodiversity Station, 216m, 0037'55"S 76°08'39"W, 9.ii.1999, Lot 2017, Trans 2, T. Erwin et al. Canopy fogging bare leaves, some with bryophytic/lichenous coat; Restrictions Apply NMNH-DCB/EPN, Agreement 39. Paratypes: 3♀ (2♀ held in trust at USNM); same as holotype, but 9.ii.99, Lot 2000, Trans 1; ECUADOR: Napo: Reserva Etnica Waorani, Transect Ent., 1km S. Okone Gare Camp, 0039'10"S 76°26'00"W, 220m,

5.ii.1996, T. Erwin *et al.* Canopy fogging, t3..3, #1423; Restrictions Apply NMNH-DCB/EPN, Agreement 39; PERU: Loreto, Explomapo Camp, Riio Napo, Rio Suscari, 15.vi.1996, 03 15°S 072° 55'W, Lot #382, T. L. Erwin, hand. coll. (♀ USNM).

***Khamul lanceolatus* Gates, n. sp.**

(Figs. 4, 16, 18, 20, 30, 58; variants: 59–64)

Etymology: *lanceolatus* (Latin, adjective) = a descriptor meaning lancelike, referring to the mandible.

Diagnosis and identification: Tegula brownish, apical mandibular tooth narrow, almost linear. Preorbital carinae finely produced ventrally but not delimiting a reniform subocular fovea, not produced as a triangular process between lateral ocellus and eye (Fig. 60). Marginal venation shorter than in other species of *Khamul* (Fig. 31) and is bordered anteriorly by a membranous strip. Propodeal median channel distinctly delimited (Fig. 64) and the posterior invagination of the dorsellum is bisected.

Description: Female holotype. Length 5.3 mm. Head, antenna, body, and coxae black. Tegula pale brown. Legs black except for tibiae, tarsi and apical third of femora yellow. Pretarsus brown. Fore wing hyaline, venation brown.

Head. 1.43X as broad as high; 1.2X wider than pronotum; HTE:msp 3.40. POL 5.7X as long as OOL. Width of oral fossa 0.36X width of head. Clypeus separated from supraclypeal area by carina. Preorbital carina of uniform width beneath eye, reniform subocular fovea absent, carina not produced as triangular tooth at vertex. Scape 3.33X as long as broad. Antennal segment relative measurements 40:6:1:26:19:19:17:16:15:32. Clava 1.88X as long as broad.

Mesosoma. Dorsal pronotum 1.74X as broad as long. Mesoscutal midlobe 0.75X as broad as long. Scutellum 0.67X as broad as long; broadly convex dorsally, scutellar boss present, subequal in dimensions to two adjacent umbilicate puncta and surrounding border combined. Dorsellum disc composed of a central -shaped structure, depressed dorsally, connected laterally to submedian carinae (Fig. 4); posterior invagination bisected by carina. Propodeal median channel distinct, delimited laterally by carinae, composed of quadrate/rectangular foveae (Fig. 4), channel bordered laterally by smaller, but distinct punctae. Relative measurements marginal:postmarginal:stigmatal veins as 20:28:20; stigmal vein straight (Fig. 31).

Metasoma. Petiole 4.0X as broad as long in dorsal view; anterolaterally protuberant, anterior carinae weak; transverse ventral carina present basally, abutted by carinae and grooves (Fig. 59). Gastral terga measurements in dorsal view on median line as 15:32:50:40:16:6, syntergum not visible in dorsal view.

Male. Unknown. Extralimital male known, see below.

Variation. No appreciable variation in the type material.

Biology. The specimen from Mexico bears a label indicating that it was reared from an egg of *Prisopus* Gray (Phasmatodea: Prisopodidae) associated with a leaf of *Chamaedorea* sp. (Arecaceae). Apparently, the specimen was reared at the San Antonio port-of-entry under some type of isolation. This record would not be a first phasmid egg parasitoid for the superfamily (Eady 1956), but it would be the first for the Eurytomidae.

Type material (2♀). Holotype: ♀ (INBio); COSTA RICA: Guanacaste: Est. Murcilago, 8km S.O. de Cua-jiniquil, 100m, 10–28.x.1993, L N 320300_347200, # 2403; COSTA RICA INBIO CRI001672408. Paratype: ♀ (USNM; dissected, SEM stub); same as for holotype.

Other material examined (2♀). COSTA RICA: San José: Ciudad Colón, 800m, iv–v.90, col. Luis Fournier (♀ MZCR); MEXICO: intercepted at San Antonio, TX, 13.vii.1976; ex *Prisopus* egg, *Chamaedorea* leaf; n. genus – small prepectus!" det. E. Grissell, 1978; "near *Neorileya* det. E. Grissell, 1996 (♀ USNM); PERU: Loreto, Explomapo Camp, Riio Napo, Rio Suscari, 15.vi.1996, 03 15°S 072° 55'W, Lot #382, T. L. Erwin, hand. coll. (♀ USNM).

Discussion and extralimital specimens. *Khamul lanceolatus* differs from other species of *Khamul* by the

presence of an incomplete procoxal carina anteroapically that forms a partial shelf to receive the head. This condition is intermediate between other *Khamul* species that have only a faint carina/change of sculpture and members of *Philolema s.l.*, *Aximopsis s.l.*, and *Chryseida*, etc. that possess a complete carina. Also, *K. lanceolatus* does not possess deep notauli as in other species of *Khamul*. One male closely resembling *K. lanceolatus* has been examined. This specimen is from a disparate Neotropical localities and different enough from the type material that caution is warranted before ascribing it to a specific hypothesis before enough material is at hand to understand intraspecific/sexual variation. Below, the label data for this specimen and brief differential diagnostics are reported.

BRASIL: Par: Oriximin, Alcoa Mine Rao, Rio Trombetas; 7–25.x.82, Rafael, Binde & Vidal, CDC Malaise; 00200087 (1♂ INPA). This unassociated male possesses pronounced preorbital carinae that create a concave habitus in dorsal view (Fig. 60), funiculars produced apicoventrally as sharp subtending flange (Figs. 61–63), apical margin of the clypeus is arcuate, propodeal sculpture distinctly different medially (Fig. 64), lateral panel of propodeum spanned by six carinae, petiole produced anterolaterally as angular flanges as well as anteromedially as sharp, medially pointed carina. As no other males are known in this potential “*lanceolatus* species group, male species-group versus specific characters cannot be separated. However, males of other species of *Khamul*, in general, do not possess such outstanding preorbital carinae (cf. Figs. 38, 44), funiculars may be produced but not to the extent described above (cf. Fig. 69), extreme apex clypeus emarginate (cf. Fig. 15), propodeal sculpture different (cf. Figs. 46, 56), lateral panel propodeum with umbilicate punctation, and petiole not flared anterolaterally (cf. Fig. 53).

With respect to *K. lanceolatus*, this specimen is currently placed in *Khamul* but initially was suspected to be a new genus near *Khamul*.

***Khamul tolkeini* Gates, n. sp.**

(Figs. 54–57)

Etymology. *tolkeini* (Latinized, noun) = genitive, singular, masculine; named in honor of J. R. R. Tolkein for his profound impact on the fantasy literature genre.

Diagnosis and identification. Tegula brown, hind tibia black. Preorbital carinae robustly protruding ventrally, delimiting a reniform subocular fovea (Fig. 54), furthermore, carinae expanded dorsally as triangular processes between lateral ocellus and eye (Fig. 54). Propodeal median channel distinctly delimited, composed of transverse reniform punctae, bordered laterally by smaller punctae and irregular rugosity (Fig. 64).

Description. Female Holotype. Length 3.3 mm. Head, body, and coxae black. Scape black; pedicel black basally, brown apically; flagellum dark brown. Femora, metatibia, metatarsomeres 1+2 black; pro- and mesotibiae and tarsomeres, extreme apex of metafemur, and metatarsomeres 3–5 brown (Fig. 55).

Head. 0.78X as broad as high; 1.1X wider than pronotum; HTE:msp 1.81. POL 2.5X as long as OOL. Width of oral fossa 0.42X width of head. Preorbital carina of uniform width, widening beneath eye, reniform subocular fovea present, carina produced as triangular tooth at vertex (Fig. 54). Scape 3.0X as long as broad. Antennal segment relative measurements 39:7:1:40:31:30:20:35:21:35. Clava 2.33X as long as broad.

Mesosoma. Dorsal pronotum 1.96X as broad as long. Mesoscutal midlobe 1.1X as broad as long. Scutellum 0.71X as broad as long; broadly convex dorsally, scutellar boss present, ~2.0X larger than any adjacent umbilicate puncta and its surrounding border combined. Dorsellum disc composed of a central -shaped structure connected laterally to submedian carinae (Fig. 56). Propodeal median channel composed of transverse reniform punctae, channel bordered laterally by smaller punctae and irregular rugosity (Fig. 56). Relative measurements marginal:postmarginal:stigmatal veins as 13:35:32; stigmatal vein evenly arcuate (Fig. 57); infuscation darkest along venation, fading toward disc margins.

Metasoma. Petiole 3.0X as broad as long in dorsal view; fine transverse carina anteriorly, protruberant lat-

erally; bicarinate ventrally, defining triangular fovea, produced in lateral view. Gastral terga measurements in dorsal view on median line as 15:25:45:30:10:2, syntergum not visible in dorsal view.

Male. Unknown.

Variation. The type series exhibits very little variation.

Type material (1♀). Holotype: ♀ (held in trust at USNM); ECUADOR: Orellana: Tiputini Biodiversity Station, 216m, 0037°55'S 76°08'39"W, 9.ii.1999, Lot 2016, Trans. 2, T. Erwin et al. Canopy fogging bare leaves, some with bryophytic/lichenous coat; Restrictions Apply NMNH-DCB/EPN, Agreement 39. Paratype ♀: PERU: Loreto, Explomapo Camp, Riio Napo, Rio Suscari, 15.vi.1996, 03° 15'S 072° 55'W, Lot #382, T. L. Erwin, hand. coll. (♀ USNM).

Acknowledgements

We thank Terry Erwin (Smithsonian Institution, Department of Entomology) for making his canopy-fogging residues available for examination. Thanks to Mike Sharkey (University of Kentucky) for specimens from his Colombian biodiversity work (NSF DEB-9972024). John Brown (Systematic Entomology Laboratory [SEL], PSI, ARS, USDA), Matt Buffington (SEL), Thomas Henry (SEL), David Smith (SEL, retired), Gérard Delvare (CIRAD, Montpellier, France), and Paul Hanson (University of Costa Rica, San Pedro) provided suggestions for improving this paper. Thanks also to Jeffrey Chiu (SEL) and Helen Vasaly (University of Virginia) for specimen imaging and to Scott Whittaker (Lab Manager, Scanning Electron Microscopy Lab, SI, NMNH) for stub coating and SEM access.

Literature cited

- Bolte, K. (1996) Techniques for obtaining scanning electron micrographs of minute arthropods. *Proceedings of the Entomological Society of Ontario*, 127, 67–87.
- Bouček, Z. (1988) *Australasian Chalcidoidea (Hymenoptera). A Biosystematic Revision of Genera of Fourteen Families, with a Reclassification of Species*. CAB International, Wallingford, Oxon, U.K., Cambrian News Ltd; Aberystwyth, Wales. 832 pp.
- Bugbee, R. (1936) Phylogeny of some eurytomid genera. *Entomologica Americana*, 26, 169–223.
- Burks, B. (1971) A synopsis of the genera of the family Eurytomidae (Hym., Chalcidoidea). *Transactions of the American Entomological Society*, 97, 1–89.
- Campbell, B., Heraty, J., Rasplus, J.-Y., Chan, K., Steffen-Cambell, J., & Babcock, C. (2000) Molecular systematics of the Chalcidoidea using 28S-D2 rDNA. Pp. 59–73. In Austin, A.; Downton, M. (eds.), *Hymenoptera Evolution, Biodiversity and Biological Control*, CSIRO Publishing, Collingwood, Australia, 466 pp.
- DiGiulio, J. (1997) Family Eurytomidae, pp. 477–497. In Gibson, G., Huber, J. & J. Woolley (eds.), *Annotated Keys to the Genera of Nearctic Chalcidoidea (Hymenoptera)*. NRC Research Press, Ottawa, Ontario, Canada, xi + 794 pp.
- Eady, R.D. (1956) Two new species of the genus *Paranastatus* Masi (Hym. Eupelmidae) from Fiji. *Bulletin of Entomological Research* 47(1), 61.
- Erwin, T. L., Pimienta, M. C., Murillo, O. E., & V. Aschero. (2005) Mapping patterns of -diversity for beetles across the Western Amazon basin: a preliminary case fo improving inventory methods and conservation strategies. *Proceedings of the California Academy of Sciences*, 56 (Supplement No. 1), 72–85.
- Gates, M. (2008) Species Revision and Generic Systematics of World Rileyinae. *University of California Press Publications in Entomology* 127, 342 pp.
- Gates, M. & Hanson, P. (2006) Familia Eurytomidae, pp. 380–387. In Hanson & Gauld [eds]. *Hymenoptera de la Region Neotropical. Memoirs of the American Entomological Institute* 77, 1–994.
- Gates, M., Metz, M. & Schauff, M. (2006) The circumscription of the generic concept of *Aximopsis* Ashmead (Hymenoptera: Chalcidoidea: Eurytomidae) with the description of seven new species. *Zootaxa* 1273, 9–54.
- Gibson, G. (1997) Morphology and Terminology, pp. 16–44. In Gibson, G., Huber, J. & J. Woolley (eds.), *Annotated Keys to the Genera of Nearctic Chalcidoidea (Hymenoptera)*. NRC Research Press, Ottawa, Ontario, Canada, xi + 794 pp.
- Goulet, H. & Huber, J. (Eds) (1993) *Hymenoptera of the World: an Identification Guide to Families*. Publication 1894/E,

- Research Branch, Agriculture Canada, Ottawa, Canada, vii + 668 pp.
- Grissell, E. (1995) Toryminae (Hymenoptera: Chalcidoidea: Torymidae): a Redefinition, Generic Classification and Annotated World Catalogue of Species. *Memoirs on Entomology, International* 2, 474 pp.
- Harris, R. (1979) A glossary of surface sculpturing. *Occasional papers in Entomology*, no. 28. California State Department of Food and Agriculture, Sacramento, California, 31 pp.
- Heraty, J. & Hawks, D. (1998) Hexamethylsilazane – a chemical alternative for drying insects. *Entomological News*, 109, 369–374.
- Lotfalizadeh, H., Delvare, G. & Rasplus, J.Y. (2007) Phylogenetic analysis of Eurytominae (Chalcidoidea: Eurytomidae) based on morphological characters *Zoological Journal of the Linnaean Society* 151, 441–510.
- Philips, W. (1917) Report on *Isosoma* investigations. *Journal of Economic Entomology* 10(1), 139–146.
- Philips, W. (1927) *Eurytoma parva* (Girault) Phillips and its biology as a parasite of the wheat jointworm, *Harmolita tritici* (Fitch). *Journal of Agricultural Research* 34(8), 743–758.
- Sela, J. & Boyde, A. (1977) Cyanide removal of gold from SEM specimens. *Journal of Microscopy* 111, 229–231.
- Sorenson, M.D. & Franzosa, E. A. (2007) TreeRot, version 3. Boston University, Boston, MA.
- Swofford, D.L. (2002) PAUP*. Phylogenetic Analysis Using Parsimony (*and Other Methods). Version 4. Sinauer Associates, Sunderland, Massachusetts.
- Tolkein, J. R. R. (1977) *The Silmarillion*. Allen & Unwin, U. K., 365 pp.
- Tolkein, J. R. R. (1980) *Unfinished Tales of Nmenor and Middle-Earth*, C. Tolkein (ed.). George Allen & Unwin, U.K., 480 pp.
- Wijesekara, A. (1997) Phylogeny of Chalcididae (Insecta: Hymenoptera) and its congruence with contemporary hierarchical classification. *Contributions of the American Entomological Institute*, 29 (3), 61 pp.
- Zerova, M. (1978) Hymenoptera Parasitica. Chalcidoidea – Eurytomidae. *Fauna Ukraini* 11, 1–465.
- Zerova, M. (1988) The main trends of evolution and the system of chalcids of the family Eurytomidae (Hymenoptera, Chalcidoidea). (In Russian with English summary.) *Entomologicheskoe Obozrenie*, 67, 649–674 [English translation: *Entomological Review* (1989) 68: 102–128].